Characterization of microglia in the rat subventricular zone after neonatal hypoxia-ischemia

Inauguraldissertation

zur

Erlangung der Würde eines Doktors der Philosophie

vorgelegt der

Philosophisch-Naturwissenschaftlichen Fakultät

der Universität Basel

von

Urs Fisch

aus Egnach (TG)

Basel, 2017

Genehmigt von der Philosophisch-Naturwissenschaftlichen Fakultät
auf Antrag von

Prof. Dr. Markus Rüegg (Fakultätsverantwortlicher)
Prof. Dr. Raphael Guzman (Dissertationsleiter)
Prof. Dr. Nicole Schaeren-Wiemers (Korreferentin)

Basel, den 18.04.2017

Prof. Dr. Martin Spiess
Dekan

meinen Eltern gewidmet

Characterization of microglia in the rat subventricular zone after neonatal hypoxia-ischemia

Content

1. Acknowledgements 6

2. Abstract 7

3. Introduction 8
3.1. Clinical perspective on neonatal HI 8
3.2 The Rice-Vannucci model of HI to study ischemia-induced neurogenesis in the postnatal SVZ 9
3.3. The role of microglia in brain development and postnatal neurogenesis 11
3.3.1. Microglial origin and maintenance 11
3.3.2. Microglia in the developing CNS 14
3.3.3. Microglia and neurogenesis 17
3.3.4. Microglia and neonatal HI 23
3.4. The aim of this study 26

4. Methods 27
4.1. Animals 27
4.2. HI surgery 27
4.3. BrdU administration and brain collection for stainings 27
4.4. Cresyl violet staining and selection of animals with ipsilateral brain injury 28
4.5. Immunohistochemistry 29
4.6. Brain section image acquisition and analysis 29
4.6.1. SVZ area and microglial quantification 30
4.6.2. Quantification of cell proliferation and microglial ball-and-chain phagocytosis 30
4.7. SVZ microglia isolation and RNA purification 31
4.8. Microglial transcriptome analysis 32
4.9. Quantitative real-time PCR validation 33
4.10. Primary neurosphere generation from SVZ tissue and microglial depletion 33
4.11. Immunocytochemistry 34
4.12. Cell culture image acquisition and analysis 34
4.13. Flow cytometry 35
4.14. Statistical analysis 35

5. Results 36
5.1. SVZ transiently enlarges while NPC density remains unaltered after HI 36
5.2. SVZ microglia specifically accumulate and remain activated after HI 38
5.3. SVZ microglia proliferate early after HI 41
5.4. HI temporarily increases the proportion of amoeboid SVZ microglia 42
5.5. Increased number of ball-and-chain phagocytic SVZ microglia after HI 43
5.6. SVZ microglia upregulate pro- and anti-inflammatory and neurotrophic genes after HI 45
5.7. SVZ microglia are not polarized to M1 or M2 after HI 49
5.8. SVZ microglial transcriptome is enriched for neurodegenerative pathways after HI 50
5.9. Microglial depletion reduces neurosphere formation 52

6. Discussion 58
6.1. Sustained accumulation and prolonged activation of SVZ microglia after HI 58
6.2. Early SVZ microglial proliferation is increased by HI 60
6.3. SVZ microglia remain phagocytic after HI 60
6.4. SVZ microglia express neurotrophic and immunomodulatory genes early after HI 62
6.5. SVZ microglia do not adopt a M1 or M2 polarization after HI 63
6.6. SVZ microglia transiently upregulate neurodegeneration-associated genes after HI 64
6.7. SVZ microglia support neurosphere generation in vitro 65

7. Conclusions 67

8. References 69

9. Abbreviations 77

1. Acknowledgements

This work was accomplished under the supervision of Prof. Raphael Guzman in the laboratory of 'Brain Ischemia and Regeneration' at the Department of Biomedicine, University Hospital Basel.

The project was financially supported by the Swiss National Science Foundation, the Department of Neurosurgery and the Department of Surgery, University Hospital Basel.

This thesis would not have been possible without the continuous support of numerous people for which I am deeply grateful.

First and foremost, I would like to express my gratitude to Prof. Raphael Guzman for giving me the opportunity to perform my MD-PhD thesis in his laboratory. I deeply thank Raphael for his continuous support and confidence in me, and the true academic freedom he permitted. Raphael is a devoted neurosurgeon *and* scientist and even in the most stressful time, encounters each challenge with a smile - a combination which impresses me to the core.

I would also like to thank the members of my thesis committee, Prof. Nicole Schaeren-Wiemers and Prof. Markus Rüegg, for their support and commitment.

I would especially like to thank Dr. Catherine Brégère, for her significant contributions, especially during the preparation of this manuscript, and her patience with me during our numerous productive discussions.

I would further like to thank all current and past members of the Guzman laboratory for constructive discussions, a pleasant atmosphere and excellent assistance, as well as Dr. Michael Abanto, and Dr. Florian Geier for their helpful collaboration.

2. Abstract

Background

Recent findings indicate a regulatory role of microglia on neurogenesis in the subventricular zone (SVZ). SVZ microglia in the adult rat are sought to adopt a supportive phenotype after ischemic stroke. Early postnatal microglia are endogenously activated and may therefore express an increased sensitivity to neonatal hypoxia-ischemia (HI). Therefore, we sought to investigate the impact of HI on the microglial phenotype in the early postnatal SVZ.

Methods

Postnatal-day (P)7 rats underwent sham or right-hemispheric HI surgery. Microglia in the SVZ, the adjacent cortex and the corpus callosum were immunohistochemically analyzed at P10, P20 and P40. Further, the transcriptome of SVZ microglia isolated at P10 and P20 was analyzed. Lastly, the effect of P10 microglia on *in vitro* neurosphere generation was investigated.

Results

The SVZ microglial response upon HI, characterized by cellular accumulation, prolonged activation and phagocytosis, is SVZ-specific and does not occur in adjacent brain regions. At the transcriptomic level, SVZ microglia adopt a complex phenotype, that resembles neither the M1 or M2 polarization state, but instead shares commonly expressed genes with microglia in neurodegenerative diseases. Finally, SVZ microglia appear to show trophic support for neurosphere generation *in vitro* in a concentration dependent manner.

Conclusions

Microglia are an inherent cellular component of the early postnatal SVZ and undergo specific developmental changes that are disrupted by neonatal HI injury. The SVZ microglial response to HI is complex and beyond a simplified pro- or anti-inflammatory phenotype. Our findings represent a solid basis for future research on SVZ microglia.

3. Introduction

3.1. Clinical perspective on neonatal HI

Neonatal encephalopathy is a clinically defined syndrome of disorders of neonatal brain function. It has an estimated incidence of 3 per 1000 live birth. However, neonatal encephalopathy is still missing an universally accepted definition because its etiologies are numerous and the clinical manifestation highly depends on the maturation stage of the newborn (Kurinczuk et al., 2010).

Hypoxic-ischemic encephalopathy (HIE) represents a sub-category of neonatal encephalopathy. HIE has an estimated incidence of 1.5 per 1000 live births and is by definition caused by intrapartum asphyxia (Kurinczuk et al., 2010). It accounts for 25 % of developmental disabilities in children (Shevell et al., 2000) and is one of the most common causes of morbidity and mortality in term and preterm neonates, accounting for 23 % of neonatal deaths worldwide (Lawn et al., 2005). Patients with HIE typically present with one of two injury patterns: i) the basal ganglia-thalamus pattern with injuries affecting the deep gray nuclei and perirolandic cortex or ii) the watershed predominant pattern with injuries localized in the white matter and cortex within the vascular cerebral watershed zones (i.e. the border zones between the vascular territory of the anterior and middle cerebral artery, or between the middle and posterior cerebral artery, respectively). Patients with the basal ganglia-thalamus pattern most commonly suffer from cerebral palsy, dysarthria, visual impairment and epilepsy, whereas patients with the watershed predominant pattern are prominently affected by cognitive impairment and epilepsy (Pimentel-Coelho et al., 2012).

The development of HIE can be divided into three consecutive phases: The first phase is characterized by an acute energy depletion in hypoxic brain cells and subsequent apoptosis and necrosis. The second phase is dominated by successive brain injuries which are caused by excitotoxicity (excessive extracellular accumulation of glutamate), mitochondrial breakdown, reactive oxygen / nitrogen species, and an inflammatory reaction by the immune system.

A third phase, defined by a chronic inflammatory state, is suggested to worsen outcome, predispose to further injury, or reduce repair and regeneration (Fleiss and Gressens, 2012).

Up to date, the only established therapeutic intervention for HIE is hypothermia, a relatively unspecific neuroprotective treatment, which attenuates the second phase of HIE. If started within 6 hours after birth, hypothermia successfully reduces morbidity and mortality among patients with HIE (Shankaran et al., 2012). Further, various neuroprotective (e.g. administration of erythropoietin) or neuroregenerative strategies (e.g. administration of mesenchymal stem cells or neurotrophic molecules) are evaluated in clinical trials (Pimentel-Coelho et al., 2012).

In the reaction following HIE, microglia were considered to be the main inflammatory amplifier and thus promoting damage (Khwaja and Volpe, 2008; Kaur et al. 2013). However, recent studies underscore the complex response of microglia to injury, which includes also neuroprotective and neuroregenerative features (Alvarez-Díaz et al., 2007; Hagberg et al., 2015).

3.2 The Rice-Vannucci model of HI to study ischemia-induced neurogenesis in the postnatal SVZ

In basic research, the term neonatal hypoxia-ischemia (HI) is often used as a synonym for HIE, although clear definitions of HI are pending. Several animal models of neonatal HI have been developed. Among them, the Rice-Vannucci model, first described in 1981 by Rice and colleagues, is the most commonly used. In brief, the right common carotid artery (CAA) in a 7-day old Sprague-Dawley rat is permanently ligated, followed by exposure of the animal to an 8 % oxygen / 92 % nitrogen gas mixture for 3.5 h at 37 °C. This procedure reproduces features of HIE, such as striatal and cortical damage as well as subcortical and periventricular white matter injury in the brain hemisphere ipsilateral to the CAA ligation. The 7-day old rat brain is thought to reflect the late gestational conditions in the human brain. A major disadvantage of this

model is the extensive variability of injury size among individuals, despite close adherence to procedure protocols (Fig. 1). Adaptation to other rat strains and mice as well as adjustments to individual laboratory settings resulted in various modifications of the original Rice-Vannucci model, but the essential combination of CAA occlusion, followed by exposure to hypoxia, remained (Ngyuen et al., 2015).

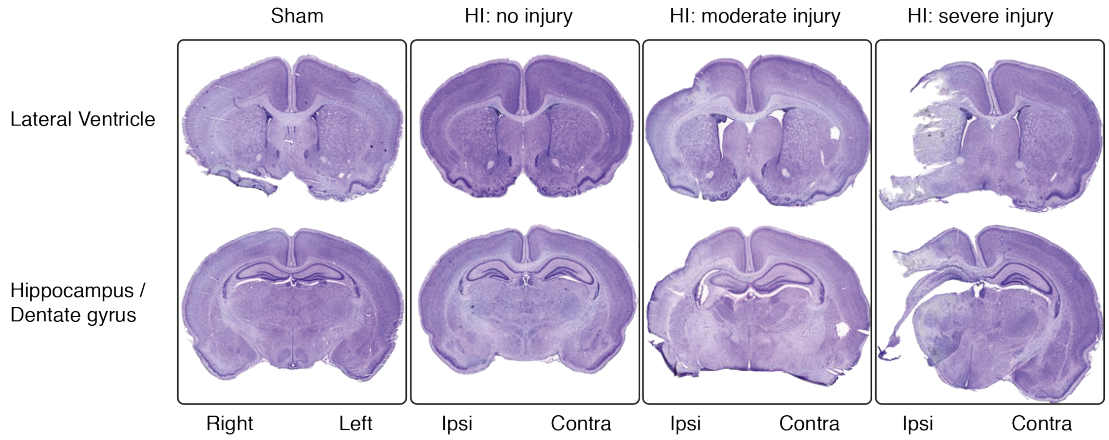

Figure 1: Representative cresyl violet stainings of brain sections from 10-day old rats that underwent sham or HI surgery 3 days before. The degree of HI injury demonstrates a marked variability among different animals (modified, from C. Brégère).

The Rice-Vannucci model and its modifications do not only enable to study the pathological features of HI injury, but also endogenous regenerative processes of the neonatal brain, specifically ischemia-induced neurogenesis in the subventricular zone (SVZ). The SVZ is a cellularly dense structure surrounding the lateral ventricles and contains a population of neural stem cells (NSC). In the postnatal rodent SVZ, NSC continuously give rise to neural progenitor cells (NPC) which migrate along the rostral migratory stream to the olfactory bulb, where they differentiate into interneurons (Zhang et al., 2008). Studies in the adult rodent demonstrated that acute ischemic stroke induces SVZ enlargement and NPC proliferation with consecutive migration of NPC from the SVZ towards the ischemic lesion (Arvidsson et al., 2002; Parent et al., 2002; Thored et al., 2006). Hence, studies in models of neonatal HI injury in mice (Plane et al., 2004) and rats (Ong et al., 2005, Yang & Levison, 2006) confirmed that the identical processes of SVZ enlargement, increased NPC proliferation

and migration towards the injury also occur after neonatal HI.

Thus, ischemia-induced neurogenesis - the enhanced NPC proliferation and migration from the SVZ - is considered a promising target for therapeutic strategies to improve recovery after brain injury.

3.3. The role of microglia in brain development and postnatal neurogenesis

3.3.1. Microglial origin and maintenance

Microglia are the resident tissue macrophage of the central nervous system (CNS) and essential to maintain homeostasis in health and to initiate immune responses in disease. They belong to the 4 most common cell types present in the brain, the others being neurons, astrocytes and oligodendrocytes. Although microglia together with astrocytes and oligodendrocytes are collectively called neuroglia (or simply glia), microglia do not derive from the neuroectoderm and migrate to the CNS during early embryogenesis (Ginhoux et al., 2010).

Microglia are distributed throughout the adult brain and spinal cord and represent about 10 % of the non-neuronal cell population with prominent regional differences in both the rodent (Lawson et al., 1990) and human brain (Mittelbronn et al., 2001).

Although microglia had already been described earlier as "pathological cells" in various brain diseases by Karl Frommann, Franz Nissl, Alois Alzheimer and others, a silver carbonate impregnation staining modified by del Rio-Hortega (1882 - 1945) represented a break-through in their identification as a unique cell type (del Rio-Hortega, 1932). Del Rio-Hortega's studies between 1919 and 1927 were the basis for his landmark publication "Microglia" in 1932. In this article, del Rio-Hortega did not only introduce microglia as a distinct cell

type in the CNS, he also presented several fundamental postulates on microglia that were visionary at that time (del Rio-Hortega, 1932). In summary, he described microglia as amoeboid-shaped cells of mesodermal origin, which populate the CNS during early development and while the brain matures, adopt a tree-like ramified morphology. Upon pathological events, microglia react by acquiring a phenotype reminiscent to the early developmental stage, which is characterized by cellular proliferation, migration to the site of damage and phagocytosis (Kettenmann et al. 2011). Remarkably, these hypotheses, introduced almost a century ago, have all been confirmed and remain current. Among them, the microglial origin was the subject of most debate.

Pio del Rio-Hortega, together with Santiago Ramon y Cajal and William Ford Robertson, already suspected that microglia are of mesodermal origin, although their assumptions were largely ignored by the scientific community. Instead, the majority agreed for decades that microglia derive from the neuro-ectoderm. Nevertheless, del Rio-Hortega's original hypothesis gained popularity through major discoveries such as phenotypic homologies between microglia and macrophages (Perry et al., 1985) and microglial necessity for PU.1, an essential transcription factor for myeloid cell production (McKercher et al., 1996). Although the myeloid origin of microglia became accepted, it was still unknown how these cells populate the CNS. For a long time, microglia were thought to derive from bone marrow (BM)-derived circulating blood monocytes and to be continuously replaced throughout life. However, immunohistochemical (IHC) studies in the fetus showed that myeloid cells invade the brain as early as on embryonic day (E) 8.5 in rodents (Alliot et al., 1999) and 4.5 weeks of gestation in humans (Monier et al., 2007), which is at a time before BM hematopoiesis begins. Indeed, fate-mapping studies revealed that microglia actually derive from primitive myeloid progenitors in the yolk sac before E8 (Ginhoux et al., 2010) that migrate to the developing brain before the blood brain barrier (BBB) establishes. Furthermore, the transcription factor Myb was found to be required for the development of hematopoietic stem cells from E10.5 on, but not for the primitive hematopoiesis in the yolk sac. Accordingly, mice lacking Myb developed normal microglia but not BM-derived monocytes

(Schulz et al., 2012). Thus, microglia and BM-derived monocytes represent two different myeloid cell populations.

However, the question remained if monocytes may still contribute to a certain extent to the microglial pool after birth. Indeed, earlier studies using BM chimeras suggested that BM-derived stem cells can invade the CNS after whole-body irradiation and adopt a microglia-like phenotype (Priller et al., 2001). However, whole-body radiation was found to impair the BBB which potentially confounded these results. In consequence, studies that did not damage the BBB by avoiding irradiation of the head (Mildner et al., 2007) or by combining parabiosis with myeloablation (Ajami et al., 2007; 2011) did not show long-term contribution of infiltrating monocytes to the microglial pool.

Recently, an elegant genetical system was developed for microglial depletion without the need for myeloablation. Briefly, a mouse line, in which tamoxifen-inducible Cre-recombinase is expressed under the control of the fractalkine receptor (CX3CR1) promotor, was crossed with a Cre-inducible diphtheria toxin receptor (iDTR) mouse line. In these CX3CR1^{CreER}:iDTR mice, tamoxifen injections induced diphtheria toxin receptor expression specifically in CX3CR1+ microglia, which were subsequently depleted by diphtheria toxin administration. After conditional depletion, CNS-resident microglia, but not peripheral monocytes, repopulated the brain within 5 days by extensive proliferation involving interleukin (IL)-1 receptor signaling (Bruttger et al., 2015). Thus, microglia populate the CNS during early embryogenesis as a distinct group of myeloid cells and maintain the capacity for self-renewal under physiological conditions without involvement of BM-derived progenitor cells.

Certain CNS inflammatory conditions accompanied with massive BBB breakdown, such as ischemic stroke, recruit monocytes to the site of injury where they transform to tissue macrophages. However, little is still known about the long-term fate of these tissue macrophages and if they become integrated in the microglial network or are only a temporary addition. Attempts to address these questions are hampered by the fact that tissue macrophages and microglia could hitherto not be distinguished by IHC stainings. Recent findings in CX3CR1$^{GFP/+}$CCR2$^{RFP/+}$ BM-chimeric mice (with unaltered CX3CR1$^{+/+}$

microglia) undergoing ischemic stroke demonstrated a restricted perilesional presence of CX3CR1$^{GFP/+}$ tissue macrophages until 28 days after the injury (Garcia-Bonilla et al., 2016), indicating that tissue macrophages persist in the CNS for at least one month after ischemia.

3.3.2. Microglia in the developing CNS

Historically, microglia were known as mediators of inflammation. Consequently, ramified microglia in the healthy adult brain were thought to reflect a stable "resting-quiescent" phenotype and become activated only under pathological circumstances. In a pivotal study using *in vivo* two-photon microscopy, Nimmerjahn and colleagues (2005) demonstrated that ramified microglia are actually highly dynamic by constant extension and retraction of their cellular processes and hereby physically interact with their neighbouring cells. This unexpected finding gave rise to a series of fascinating discoveries on the sculpturing role of microglia in the healthy brain, especially during CNS development. On the other hand, these findings also pointed out how critically dependent brain development is on properly functioning microglia.

Microglia colonize the developing brain as early as E8.5 (Ginhoux et al., 2010), before the CNS will undergo extensive developmental changes. The early presence of microglia in the developing brain raised the question if microglia participate in neurodevelopment. A prominent feature of early CNS development is selection of redundant newborn cells through programmed cell death (Burek and Oppenheim, 1996). Indeed, microglia are a key player involved in this process by inducing apoptosis and subsequently phagocytosing neuronal cells (Ferrer et al., 1990; Marin-Teva et al., 2004; Wakselman et al., 2008) via Triggering receptor expressed on myeloid cells 2 (TREM-2) / TYRO protein tyrosine kinase-binding protein (DAP12) signaling without eliciting inflammation (Takahashi et al., 2005). During the late stages of cortical neurogenesis, microglia specifically accumulate in the embryonic SVZ and phagocytose NPCs, thus actively regulating the number of NPCs in the

developing brain (Cunningham et al., 2013). In addition, observations *in vitro* where microglia contacted previously live NPCs and subsequently engulfed them (Fricker et al., 2012; Cunningham et al., 2013) led to the hypothesis that microglia may even phagocytose live cells, although the direct evidence is still pending (Brown and Neher, 2014).

Microglia are not only executors of programmed cell death, but are equally important for survival, proliferation and differentiation of NPCs via release of trophic factors such as low concentrated cytokines, including IL-1β, IL-6, tumor necrosis factor alpha (TNF-α) and interferon gamma (IFN-γ) (Shigemoto-Mogami et al., 2014) or insulin-like growth factor 1 (IGF-1) (Ueno et al., 2013). IGF-1 is a well known neurotrophic factor and affects NPCs in multiple ways, including anti-apoptotic effects (Chrysis et al., 2001), and reduces cell cycle length and increasing cell cycle reentry (Hodge et al., 2004). The microglial support of developmental neurogenesis is addressed in more detail in chapter "3.3.3. Microglial and neurogenesis".

In addition to regulation of newborn cell fate, microglia play a substantial role in establishing connectivity in the developing brain through controlled elimination of unnecessary synapses. Similar to the programmed cell death of surplus cells, synaptic connections are initially produced in excess, followed by removal of redundant or faulty synapses called 'synaptic pruning'. Microglia are temporarily enriched in brain regions undergoing synaptic refinement and contact synapses in a neuronal activity-depending manner (Wake et al., 2009; Tremblay et al., 2010; Schafer et al., 2012). Weak synapses are identified and eventually removed either via interaction of synaptic complement C1q and C3 and microglial complement receptor 3 (CR3) (Schafer et al., 2012) or via interaction of neuronal fractalkine (CX3CL1) with microglial CX3CR1 (Paolicelli et al., 2011). Perturbing the synaptic pruning has long-lasting consequences on development. Knock-out of several microglial signaling proteins (CX3CR1, CR3, DAP12) or depleting microglia with colony stimulating factor 1 receptor (CSF1R) antibodies significantly alters the outgrowth of dopaminergic axons in the forebrain and the laminar positioning of subsets of neocortical interneurons

(Squarzoni et al., 2014). Further, conditional depletion of microglia in CX3CR1^{CreER}:iDTR one-month old mice causes deficits in multiple learning tasks and learning-induced synaptic remodelling (Parkhust et al., 2013).

Lately, the different stages of microglial developmental have been extensively characterized using genome-wide expression profiling (Matcovitch-Natan et al., 2016). Murine microglia were isolated from 9 time points, *in utero* from E10.5 until E16.5, early postnatally from postnatal day (P)3 until P9 and from the two-months old adult mouse. Global gene expression analysis revealed 3 distinct developmental stages (E10.5 - E14, E19 - P9, >P9), which are characterized by different regulatory factors (Matcovitch-Natan et al., 2016). In line with these results, another study identified transmembrane protein 119 (TMEM119) as a novel marker for adult microglia (Bennett et al., 2016). TMEM119 expression is developmentally regulated and reaches adult levels after P14. Thus, microglia in the early postnatal brain are yet *not fully maturated* and may therefore *differentially react to injury* compared to their adult counterparts.

Of note, these two recent studies analyzed early postnatal microglia on a whole-brain scale. However, earlier studies already noticed marked regional differences in microglia within the first two weeks after birth. Fascinatingly, it was once more del Rio-Hortega who described first a distinctive accumulation of amoeboid-shaped microglia restricted to the SVZ and supraventricular corpus callosum while cortical microglia already display a ramified morphology (del Rio-Hortega, 1932). Successive histological analyses characterized these amoeboid microglia as highly proliferative and phagocytic (Wu et al., 1992; Hristova et al., 2010). Importantly, in a study by Shigemoto-Mogami et al. (2014), these early postnatal SVZ microglia were shown to be highly activated (defined by their expression of the lysosomal marker CD68), and to enhance the proliferation of NPCs in the SVZ.

In conclusion, microglia are substantially involved in neurodevelopment as soon as they migrate to the brain. Concurrent to brain development, microglia undergo a step-wise maturation process themselves. Recent genome-

wide expression analyses demonstrated that murine microglia retain a developmental phenotype until the end of the second postnatal week. In particular, microglia in the SVZ are highly activated and support NPC proliferation during that early postnatal time period.

3.3.3. Microglia and neurogenesis

In the healthy mammal brain, the major neurogenic stem cell niches are the subgranular zone (SGZ) in the hippocampus and the SVZ next to the lateral ventricles.

The SGZ is a thin layer of cells, including NSCs / NPCs, forming one of several components of the dentate gyrus in the hippocampus. Throughout life, SGZ-derived NPCs migrate locally into the granular region of the dentate gyrus to differentiate into neuronal granule cells. These granule cells become then integrated in the hippocampal network, which is crucial for learning and memory functions. In brief, type-1 radial glial-like stem cells give rise to type-2 progenitor cells through asymmetrical cell division. Type-2 progenitor cells are highly proliferative and expand in numbers while eventually transforming into type-3 cells which will then exit the cell-cycle and differentiate into excitatory granule neurons that will locally integrate into the granular layer of the dentate gyrus (Kempermann et al., 2015).

The other prominent stem cell niche is the SVZ, which lines out the walls of the lateral ventricles. In contrast to neurogenesis in the SGZ, SVZ-derived neurons migrate extensively along the rostral migratory stream and differentiate into interneurons in the olfactory bulb. While the rostral migratory stream in rodents is characterized in great detail, its existence in humans is controversial. Within the SVZ, astrocyte-like type-B cells are the quiescent stem cells which generate transient amplifying type-C cells by asymmetric division. Type-C cells proliferate and give rise to the type-A NPCs which then migrate and differentiate to become neurons (Zhang et al., 2008).

Microglia are an inherent cellular component of the neurogenic niches (Sato, 2015). While originally, microglia as mediators of inflammation were thought to negatively influence neurogenesis, more recent studies brought evidence that in the healthy brain, they support neurogenesis and neuronal survival by secreted cytokines and trophic factors. However, the potentially versatile roles of microglia in the neurogenic niches after brain injury are still widely unknown.

Earlier studies about the microglial role on SGZ neurogenesis demonstrated that lipopolysaccharide (LPS)-induced acute inflammation reduces neurogenesis in the adult rat hippocampus by microglial secretion of IL-6 and TNF-α (Monje et al., 2003; Ekdahl et al., 2003). Additional studies underlined that microglial release of interleukins, including IL-1β reduce hippocampal neurogenesis in the aged rat, also without prior exposure to LPS (Gemma et al., 2007). On the other hand, hippocampal microglia were also shown to be neurotrophic in the context of different models of induced neurogenesis, including enriched environment housing, wheel running, status epilepticus or adrenalectomy (Williamson et al., 2012; Kohman et al., 2012; Gebara et al., 2013; Vukovic et al., 2012; Choi et al., 2008). Adult rats, exposed to an enriched environment, upregulate microglial ionized calcium-binding adapter molecule 1 (Iba1) expression and brain-derived neurotrophic factor (BDNF) in the hippocampus and specifically in the dentate gyrus. Interestingly, when exposed to LPS, these animals express an attenuated IL-1β and TNF-α response in the hippocampus than control animals (Williamson et al., 2012). An alternative model to induce hippocampal neurogenesis is wheel running. While wheel running induces proliferation of SGZ NPCs, it concurrently reduces the total number of SGZ microglia. However, the relative proportion of supportive IGF-1+ microglia actually increases (Kohman et al., 2012; Gebara et al., 2013). In contrast to these findings, another study did not find a decrease of hippocampal microglia after running, but also demonstrated increased neurogenesis *in vitro* which was mediated by SGZ microglia via CX3CL1-CX3CR1 signaling (Vukovic et al., 2012). Pathological events like status epilepticus can also induce hippocampal neurogenesis. Two days after a

pilocarpine-induced status epilepticus, an IGF-1 dependent increase of SGZ neuroblasts was observed. IGF-1 was mainly produced by microglia close to the SGZ (Choi et al., 2008). In a further study, adult rats underwent adrenalectomy and the subsequent deprivation of endogenous glucocorticoids resulted in NPC proliferation in the SGZ. Interestingly, this increase in neurogenesis correlated with augmented numbers of non-ramified SGZ microglia (Battista et al., 2006).

Furthermore, SGZ microglia were shown to regulate NPC numbers not only via secreted factors but also via phagocytic activity. Meticulous fate-mapping studies demonstrated that the majority of newly born SGZ NPCs undergo apoptosis within the first 4 days after division and are rapidly phagocytosed by resident microglia (Sierra et al., 2010). It is hypothesized that microglia may phagocytose live cells and thereby actively regulate neurogenesis (Brown and Neher, 2014).

Thus, different models of induced SGZ neurogenesis demonstrate that microglial numbers are linked to postnatal SGZ neurogenesis, although the results are heterogeneous. Additionally, phagocytosis of newly born NPCs is a common feature of microglia in the healthy adult hippocampus.

As previously described, neurogenesis in the SVZ and SGZ are similar but not identical. Therefore, microglia may have different functions among these two stem cell niches. In a pivotal study, Cunningham and colleagues (2013) addressed extensively the role of microglia in the SVZ during late embryonic and early postnatal development across different species. Amoeboid-shaped microglia accumulated specifically in the developing SVZ in rat, macaque and human brains *in utero* and actively regulated the number of NPCs via phagocytosis. Reducing microglial activity by administration of doxycycline or depleting microglia by liposomal clodronate markedly increased the number of NPCs, while inversely, enhancing microglial activity by LPS injection decreased it. As described in the previous chapter, microglia display an embryonic phenotype until the end of the second postnatal week before adopting an adult state (Matcovitch-Natan et al., 2016). Shigemoto-Mogami and colleagues (2014) demonstrated in a combination of *in vitro* and *in vivo* approaches that during this critical time period, downregulation of microglial activity by

minocycline (which acts similarly to doxycycline) leads to a decrease in SVZ neurogenesis via reduction of microglial-derived IL-1β, IL-6, TNF-α and IFN-γ. Interestingly, a mix of function-blocking antibodies against these 4 cytokines reproduces the effect of minocycline on neurogenesis *in vitro*, whereas inhibition of individual cytokines is insufficient. Vice-versa, addition of IL-1β and IFN-γ in low concentrations (1 ng / ml) promotes neurogenesis. Hence, the release of the right amount and combination of cytokines by microglia support early postnatal neurogenesis. In line with these results, low-dose administration of IFN-γ acts proneurogenic in the adult SVZ (Pereira et al., 2015) and pharmacological inhibition of IL-6 reduces the number of SVZ-derived neurospheres after HI (Covey et al., 2011). These findings suggest that mediators, including IL-1β, IL-6, TNF-α or IFN-γ, which are on one hand detrimental for neurogenesis in the setting of excessive inflammation (Monje et al., 2003), are on the other hand beneficial or even essential for neurogenesis if appropriately secreted within the right microenvironment.

Furthermore, *SVZ microglia may have inherent properties* which distinguishes them from microglia of other brain regions. In the adult mouse, SVZ microglia are more proliferative than microglia in the striatum or corpus callosum (Goings et al., 2006) and culturing microglia from the SVZ yields in 20 times more cells than culturing microglia from non-neurogenic brain regions (Marshall et al., 2008). However, when SVZ microglia are co-cultured with cortical tissue, their proliferative capacity is reduced, suggesting that microglia sense their environment and adapt to it (Marshall et al., 2014). Furthermore, SVZ-derived primary cell cultures, but not cerebellum-derived cultures, retain the ability for self-renewal for more than 300 passages. However, the SVZ cell cultures rapidly lose their capacity to differentiate into neuron-specific class III β -tubulin (TUJ1)+ NPCs after the tenth culture passage, which is concurrent to the depletion of primary microglial cells. On the other hand, the capacity to form neuroblasts is reconstituted in passage 300 SVZ cell cultures if they are supplemented with conditioned medium from passage 3 SVZ cultures in which microglia are still present in high numbers. Importantly, differentiating passage 3 SVZ cell cultures have significantly reduced numbers of TuJ1+ NPCs if microglia are previously depleted (Walton et al., 2006). Vice-versa,

supplementation of SVZ microglia but not cortical microglia increase the numbers of TuJ1+ NPCs in murine SVZ cultures (Marshall et al., 2014).

Further *in vitro* data point out that the neurotrophic effect of microglia depends on the mode of activation. Microglia activated by IL-4 produce high levels of IGF-1, downregulate TNF-α and promote adult NPC differentiation to oligodendrocytes, whereas low levels of IFN-γ stimulation favour neurogenesis. On the other hand, activation by LPS inhibits NPC differentiation (Butovsky et al., 2005; 2006). These findings exemplify that *microglial activation is versatile and context-dependent*. Though, generally accepted definitions of *in vivo* microglial activation states are still pending.

As previously mentioned, microglial phagocytosis is crucial for tissue homeostasis in the hippocampus (Sierra et al., 2010). "Eat-me" signals, such as phospholipid phosphatidylserine, are important for the identification and subsequent phagocytosis of apoptotic or potentially stressed but still live cells (Brown and Neher, 2014; Arandjelovic and Ravichandran, 2015). Phospholipid phosphatidylserine is a component of the plasma membrane that is normally located on the intracellular side of the cell membrane, but is externalized to the cell surface upon injury or stress. It is then recognized by the TAM receptors Mertk and Axl on microglia which induce phagocytosis. In adult wilde-type mice, the SVZ is void for the apoptotic marker cleaved-caspase-3 (CC3), underlining that microglial phagocytosis is highly efficient. However, in $Axl^{-/-}$ $Mertk^{-/-}$ mice, CC3+ cells accumulate in the SVZ and along the rostral migratory stream while bromodeoxyuridine (BrdU)+ cells in the olfactory bulb increase by 70 % (Fourgeaud et al., 2016). These findings suggest that TAM receptor-mediated microglial phagocytosis is crucial for tissue homeostasis in the SVZ and neuroblast survival along the rostral migratory stream.

Two additional aspects add even more complexity to the regulatory role of microglia on NPCs. First, neurotrophic support by microglia may not be limited to their close surrounding but may also affect remote regions. For instance, the survival of early postnatal cortical layer V neurons appears to be

directly dependent on the secretion of IGF-1 and CXCL3-CXCR3 signaling of supraventricular microglia (Ueno et al., 2013). Secondly, microglia-NPC interaction is not unilateral but reciprocal. NPCs regulate microglial proliferation, migration, and phagocytosis via the secretion of immunomodulatory proteins, including vascular endothelial growth factor (VEGF) (Mosher et al., 2012; Liu et al., 2013).

Brain ischemia temporarily induces neurogenesis by mechanisms which are still not completely understood (Zhang et al., 2008). The role of microglia in this ischemia-induced neurogenesis was so far only addressed by a few studies. Thored and colleagues (2009) showed that after a 2 h middle cerebral artery occlusion (MCAO) in the rat, SVZ microglia ipsilateral to the ischemic injury accumulate over 16 weeks with a peak at 6 weeks. These microglia express CD68, a lysosomal marker of microglial activation and neurotrophic IGF-1. The authors thus concluded that SVZ microglia support post-ischemic neurogenesis by adopting a proneurogenic phenotype. However, a similar study with only 30 min MCAO did not lead to SVZ microglial accumulation (Chapman et al., 2015), suggesting that the degree of injury is crucial for the SVZ microglial response. Interestingly, a partial depletion of SVZ microglia by intrathecal administration of anti-CD11b saporin-conjugated antibodies, followed by 2 h MCAO does neither affect the number of NPCs in the striatum nor alter their migratory distance from the SVZ (Heldmann et al., 2011). However, this depletion method does not achieve a complete eradication, because the CD11b+ microglia define only a subpopulation of all SVZ microglia. While the antibody treatment successfully reduces the number of CD11b+ microglia by 73%, it reduces the number of all SVZ microglia by only 43%. Importantly, the number of CD68+ microglia is not affected by the antibody depletion treatment.

In conclusion, there is growing evidence that microglia in the neurogenic niches play a major role in NPC regulation through phagocytosis and secretion of factors which promote neurogenesis. The interaction between microglia and NPCs seems to be considerably dependent on the microenvironment. Limited data suggests that SVZ microglia support neurogenesis after ischemic stroke in

the adult rodent. Further studies implicate that in the early postnatal SVZ, endogenously activated microglia are *per se* neurotrophic. So far, the impact of HI on SVZ microglia during this time period has not been addressed.

3.3.4. Microglia and neonatal HI

For decades, the microglial activation upon pathological stimuli was thought to reflect an uniform response with neurotoxic effects (Kettenmann et al., 2011). First evidence of such neurotoxic effects derived from *in vitro* experiments in the early 1990s, where microglia were stimulated by high concentrations of pro-inflammatory LPS, IFN-γ or TNF-α. Meanwhile, the limitations of such artificial *in vitro* experiments became evident (Hellwig et al., 2013).

Further research indicated that the microglial responses upon pathological stimuli were more diverse than previously anticipated and involved not only pro-inflammatory but also neuroprotective mechanisms. Various attempts were made to categorize the different microglial reactions into either beneficial or detrimental for the CNS. The M1 / M2 polarization paradigm for microglial characterization emerged from *in vitro* observations in macrophages. Macrophages express different sets of markers upon stimulation by T-helper cell type T_H1-derived IFN-γ or T_H2-derived IL-4. In analogy to T_H1 and T_H2 cells, the corresponding macrophage cell types are called M1 and M2, respectively. The IFN-γ induced M1 phenotype is defined as the "classical" activation, which is characterized by expression of pro-inflammatory cytokines including TNF-α, IL-1β, and IL-6, as well as induction of reactive oxygen species-generating inducible nitric oxidase (iNOS) and nicotinamide adenine dinucleotide phosphate (NADPH) oxidase. In contrast, the IL-4 induced M2 phenotype is defined as the "alternative" activation, which is characterized by secretion of anti-inflammatory cytokines, such as IL-10 and transforming growth factor-β (TGF-β), neurotrophic factors (including IGF-1 and BDNF), and induction of arginase 1 (Arg1). Due to the close similarities of microglia and macrophages, the M1 / M2 polarization paradigm was subsequently applied to microglia with

M1 activation characterized as pro-inflammatory and neurotoxic, and M2 activation as anti-inflammatory, neurogenic and regenerative (Hu et al., 2015). Consequently, this polarization paradigm is used in numerous studies on microglial characterization in the context of acute ischemia and neonatal HI (e.g. Hellström-Erkenstam et al., 2016).

However, the M1 / M2 polarization paradigm was shown to have major limitations and increasing evidence even suggests that it is inadequate to describe microglial activation *in vivo* (Ransohoff, 2016). Indeed, characteristic markers for M1 or M2 polarization derive from *in vitro* experiments and cannot be reproduced *in vivo*. In opposite, transcriptome studies of isolated microglia from various animal models of neurodegenerative diseases including Alzheimer's disease (AD) and amyotrophic lateral sclerosis (ALS) do not display a relevant tendency of microglia toward the M1 or M2 phenotype (Holtman et al., 2015). Furthermore, accumulating evidence demonstrate that microglia and macrophages co-express distinct M1 and M2 markers concurrently even at a single-cell level and that the expression pattern of M1 / M2 markers is merely random (Chiu et al., 2013; Holtman et al., 2015; Szulzewsky et al., 2015; Morganti et al., 2016; Kim et al., 2016), leading the M1 / M2 paradigm *ad absurdum.* In consequence, key opinion leaders on microglial research suggest to no longer rely on the M1 / M2 polarization paradigm when describing microglial phenotypes *in vivo* (Ransohoff, 2016; Colonna and Butovsky, 2017). Undeniably, more *in vivo* studies are needed to establish a better approach on microglial characterization.

Studies on microglia in the context of ischemia are further complicated by the fact that microglia are immunohistochemically not distinguishable from invading macrophages (Hellwig et al., 2013). Invading macrophages are thought to play a different role than microglia after ischemic injury (Ritzel et al., 2015; Kim and Cho, 2016), but little is yet known about their long-term fate in the CNS after the injury (Garcia-Bonilla et al., 2016). Importantly, conditional depletion of microglia after brain ischemia in the adult rodent leads to increased stroke size and dysregulation of neuronal network activity (Lalancette-Hebert et al., 2007; Szalay et al., 2016), suggesting that overall, microglia are rather protective than

neurotoxic after ischemia. Nonetheless, our understanding of the microglial role in ischemic stroke is still incomplete and demands further investigations.

The pathogenesis of ischemic brain injury in the early postnatal brain shares many features of that in the adult brain, but there are also significant differences due to immaturity of both the CNS and the immune system. Most noteworthy among those differences is a more rapid proliferation and accumulation of microglia / macrophages after neonatal brain injury, which is likely due to their different developmental stage (Vexler and Yenari, 2009). Thus, the microglial reaction to brain injury is greatly affected by age which needs to be considered when comparing findings among different studies.

The temporal characterization of inflammation after neonatal HI indicates a rapid inflammatory response in the CNS within the first 3 hours which lasts up to 7 months (Bonestroo et al., 2013). During this time period, microglia / macrophages are most prominent during the first two weeks after the injury (Winerdal et al., 2012). Flow cytometry analysis from a neonatal MCAO model indicate that the majority of CD11b+ CD45+ cells in the perilesional tissue are $CD45+_{low}$ microglia rather than $CD45+_{high}$ macrophages (Denker et al., 2007). By using the double transgenic mouse line $CX3CR1^{GFP/+}CCR2^{RFP/+}$, where green-fluorescent CX3CR1+ microglia can be distinguished from red-fluorescent CCR2+ macrophages, it is shown that resident microglia outnumber infiltrating macrophages in the injured hippocampus for up to 28 days after neonatal HI (Umekawa et al., 2015).

Endogenously activated microglia accumulate specifically in the periventricular white matter during mid to late gestation in humans (Billiards et al., 2006) and until the second postnatal week in rodents (Hristova et al., 2010; Shigemoto-Mogami et al., 2014). Periventricular white matter damage is a hallmark of HIE in preterm infants. Thus, the spatio-temporal accumulation of activated microglia is thought to be mainly responsible for the periventricular white matter vulnerability to hypoxia through an excessive microglia-mediated inflammatory response (Khwaja and Volpe, 2008; Kaur et al. 2013).

On the other hand, microglia promote repair and regeneration in the subacute phase after injury through phagocytosis of debris and release of

neurotrophic mediators (Alvarez-Díaz et al., 2007; Neumann et al., 2009). Importantly, depletion of microglia in a neonatal MCAO model actually increases brain injury size and the risk of post-ischemic hemorrhagic transformation, hence suggesting that the presence of microglia is rather beneficial than detrimental for the injured brain (Faustino et al., 2011; Fernandez-Lopez et al., 2016).

To conclude, until recently, the microglial role after neonatal HI was heavily influenced by the M1 / M2 polarization paradigm on microglia to adopt either an aggravating (M1) or a supportive (M2) phenotype. However, accumulating evidence strongly suggests that this categorization is rather artificial and insufficient to characterize microglial function *in vivo.* The current findings on microglia in neonatal HI remain controversial with microglia promoting damage in the acute phase and repair in the post-acute phase. More studies are needed to disassemble the numerous microglial effects in neonatal HI.

3.4. The aim of this study

Recent findings indicate that microglia in the neurogenic niches are a key modulator of neurogenesis (Sato, 2015) and are therefore a potential therapeutic target to enhance regeneration after neonatal HI. Recently, microglia were reported to adopt a supportive phenotype in the adult SVZ after ischemic stroke (Thored et al., 2009). There are however important differences between the adult and maturing brain with regard to microglial characteristics. Early postnatal microglia do not yet express an adult phenotype (Matcovitch-Natan et al., 2016; Bennett et al., 2016) and are endogenously activated in the SVZ (Shigemoto-Mogami et al., 2014). In consequence, they may respond differently than adult microglia to brain injury. So far, microglia in non-injured brain regions, including the SVZ, have not been extensively characterized after HI. Therefore, we thought to investigate the impact of HI on the microglial phenotype in the early postnatal SVZ.

4. Methods

4.1. Animals

All animal experiments were approved by the local veterinarian authorities and complied with the Swiss animal welfare guidelines. Sprague-Dawley rats were bred in-house and the day of birth was considered as P0.

4.2. HI surgery

P7 rat neonates were randomly assigned to sham or HI surgery, with a balanced representation of both sexes among the two surgery groups. One hour prior to surgery, animals were injected intraperitoneally with buprenorphine (0.03 mg / kg body weight). Anesthesia was induced with 5 % isoflurane and maintained with 3 % isoflurane during the surgery. The HI surgery consisted of a modification of the Rice-Vannucci model (Rice et al., 1981): the right CCA was exposed and temporarily clipped with a Sugita 4mm aneurysm mini clip (Mizuho) and the skin incision temporarily sutured. Animals recovered for 10 min on a heating pad and were then placed for 40 min into a hypoxic chamber constantly flushed with a 8 % oxygen / 92 % nitrogen gas mixture (2 L / min), that was immersed in a temperature-controlled water bath to maintain an air-temperature of 37.5 °C. Animals then recovered for 10 min on a heating pad and were briefly anesthetized with isoflurane for clip removal and permanent skin suture. This procedure resulted in a cortico-striatal HI injury in the hemisphere ipsilateral to the side of CAA surgery. The sham surgery consisted of CCA exposure without temporary occlusion and without hypoxia exposure.

4.3. BrdU administration and brain collection for stainings

A first group of 30 animals was used for IHC purposes (n=5 animals for sham and HI per time point, respectively). Animals received daily single intraperitoneal BrdU injections (100 mg / kg body weight, Sigma) for 3 consecutive days before sacrifice (Fig. 2A).

Animals were then sacrificed at P10, P20 or P40 to reflect acute, subacute and chronic stages after HI, under deep anesthesia by transcardiac perfusion with normal saline, followed by 4 % paraformaldehyde (PFA) in 0.1 M phosphate buffer pH 7.4 (PB). Brains were post-fixed in 4 % PFA in PB for 48 h at 4° C, cryoprotected in consecutive 15 % and 30 % sucrose solutions, embedded in OCT (Leica Biosystems) and cryosectioned. Coronal free-floating sections (30 μm) were stored at -20° C in a cryoprotectant solution (30 % ethylene glycol, 30 % sucrose in PB) until staining.

4.4. Cresyl violet staining and selection of animals with ipsilateral brain injury

Coronal brain sections (interval 180 μm) were mounted on superfrost plus slides (Menzel), stained with 0.1 % cresyl violet acetate (Sigma) and scanned (Nikon Eclipse TI-E microscope). Brain sections including the anterior SVZ between 0.40 rostral to -0.20 caudal to bregma (in P10 rats and corresponding coordinates for the P20 and P40 rats, respectively) (Khazipov et al., 2015) were investigated in this study. Two investigators (UF, CB) independently assessed HI injury using ImageJ software (Version 2.00rc.43/1.50e) and the results were averaged. The size of HI injury was calculated by subtracting the intact area in the ipsilateral hemisphere from the total area of the contralateral hemisphere (Tuor et al., 1993) in 3 serial cresyl violet sections. Only HI animals without histological signs of HI injury in the anterior SVZ were included in this study.

4.5. Immunohistochemistry

Brain sections were washed in Tris-buffered saline (TBS), incubated in blocking buffer (TBS with 2% fish gelatine, 0.3 % triton X-100, Sigma) for one hour at room temperature (RT), then incubated with primary antibodies (Table 1) overnight at 4° C in blocking buffer, washed repetitively with TBS, and incubated with the corresponding species-specific Alexa-Fluor (488, 546, 555, 647)-conjugated Donkey or Goat (H+L) secondary antibodies (ThermoFisher) in blocking buffer (1:2000) for one hour at RT. Sections were counterstained with 0.5 μg / mL DAPI (Sigma) before mounting on superfrost slides with ProLong Gold (ThermoFisher). For BrdU labelling, sections were pretreated with 2 N HCl for 30 min at RT before the blocking step. For proliferating cell nuclear antigen (PCNA) labelling, antigen-retrieval was performed for 5 min at 80° C in Target retrieval solution (Dako) before the blocking step.

Host / primary antibody	Producer	Concentration for histology	Concentration for cytology
Mouse / anti-BrdU	BD Bioscience	1:200	
Rabbit /anti-CC3	Cell Signaling	1:200	
Mouse / anti-CD68	R&D Systems	1:2000	
Guinea pig / anti-DCX	Merck Millipore	1:2500	1:2000
Rabbit / anti-Iba1	Wako	1:2000	1:1000
Goat / anti-Iba1	Abcam	1:1000	
Rabbit / anti-Ki67	Abcam	1:1000	
Mouse / anti-Nestin	Millipore		1:500
Rabbit / anti-PAX6	Biolegend	1:1000	
Mouse / anti-PCNA	DAKO	1:700	
Mouse / anti-PSA-NCAM	Abcam	1:400	
Rabbit / anti-SOX2	Abcam	1:500	

Table 1: Primary antibodies used for IHC tissue and cell culture stainings.

4.6. Brain section image acquisition and analysis

20x wide-field immunofluorescence images from brain sections were acquired on a Eclipse TI-E microscope (Nikon), and 40x confocal immunofluorescence image stacks (330 x 330 μm, 11 μm depths, step size 0.5 μm) on a CSU-W1 microscope (Visitron Systems). Representative 40x images for depicting microglial activation were acquired on a LSM 710 confocal microscope (Zeiss). All quantitative analyses were conducted in 3 brain sections

(interval 180 μm) and mean values calculated per animal. Image acquisition settings were identical for all stainings.

4.6.1. SVZ area and microglial quantification

Quantification of SVZ area and microglial morphology, density and activation was performed manually with ImageJ from wide-field IHC images. The SVZ area was defined by its DAPI+ cellular density. The microglial morphology was classified into 3 categories: i) amoeboid with roundish cellular shape without cellular processes, ii) intermediate with irregular cellular shape and short processes and iii) ramified with cellular extensions which extended at least two-fold the diameter of the microglial cell body (Fig. 6A). The microglial density was calculated as the number of Iba1+ cells per area in 3 brain regions: i) in the SVZ, ii) in a 1600 x 200 μm rectangle including layers I-VI of the M2 supplementary motor cortex (CX), and in three 150 μm squares which were symmetrically distributed in the supraventricular median corpus callosum (CC) (Fig. 4A). The expression of CD68 is a marker for microglial activation (Shigemoto-Mogami et al., 2014). Microglial activation was calculated as the number of CD68+ Iba1+ cells per total number of Iba1+ cells in each region.

4.6.2. Quantification of cell proliferation and microglial ball-and-chain phagocytosis

PCNA+ and paired box 6 protein (PAX6)+ cells in the most medial part of the dorsolateral SVZ were manually counted in a 50 μm x 50 μm square with 10 μm depth with ImageJ from confocal stack images. Only PCNA+ and PAX6+ cells being fully included within the square were counted. Microglial proliferation (number of BrdU+ Iba1+ cells per total number of Iba1+ cells) and ball-and-chain phagocytosis (number of ball-and-chain shaped phagocytic pouches per total number of Iba1+ cells) in the dorsolateral SVZ or CX were manually

quantified in 3D-reconstructed confocal stack images with Imaris software (Vers. 7.6.5, Bitplane). In Imaris, the "mask channel" function was applied to highlight BrdU+ Iba1+ cells.

4.7. SVZ microglia isolation and RNA purification

A second group of 24 animals underwent sham or HI surgery at P7 for ipsilateral SVZ microglial isolation at P10 or P20 and subsequent gene expression analysis (n=6 for sham and HI per time point, respectively). At P10 or P20, animals were deeply anesthetized and perfused with ice-cold normal saline. Brains were extracted and kept in ice-cold Hank's balanced salt solution (HBSS) (Sigma). The region of the anterior SVZ was coronally cut with sterile razor blades in 2 mm thick sections and the ipsi-dorsolateral SVZ from two sections microdissected under a dissection microscope (Leica). Dorsolateral SVZ tissue was only collected if the HI injury did not affect the ipsilateral SVZ or the adjacent median striatum / corpus callosum (microscopic assessment during preparation). SVZ tissue from individual animals was separately collected and processed at 4°C. The SVZ tissue was washed (centrifugation at 300 *g* for 5 min, followed by aspiration of the supernatant), dissociated with the papain neural dissociation kit (Miltenyi), filtered through a 40um strainer, washed again and magnetically labeled with mouse anti-rat CD11b microbeads (1:200) (Miltenyi) for 20 min. CD11b+ cells were ferromagnetically isolated using MS columns (Miltenyi) following the manufacturer’s instructions. The purity of CD11b+ sorted cells was confirmed by flow cytometry (see chapter "4.13. Flow cytometry"). Due to the very low cell yield, simultaneous flow cytometry analysis and RNA collection was not possible. Therefore, purity of isolated CD11b+ cells was confirmed from contralateral CX tissue undergoing the same isolation procedure as the SVZ tissue. Isolated CD11b+ cells were immediately processed with the Arcturus PicoPure RNA isolation kit (ThermoFisher Scientific) including DNase treatment and temporary storage at -80° C after extraction buffer treatment. RNA isolation was then completed batch-wise. RNA

integrity of all samples was measured with the RNA 6000 Pico Kit (Agilent) on the 2100 Bioanalyzer (Agilent).

4.8. Microglial transcriptome analysis

Sample preparation for microarray processing was performed externally at Life&Brain GmbH, Bonn, Germany. In brief, 500 pg total RNA per sample were reverse transcribed into cDNA using the GeneChip WT Pico Assay Kit (Affymetrix) in a two-step process according to the manufacturer's instructions. The cDNA was subsequently fragmented, labeled and hybridized to the GeneChip Rat Transcriptome Array 1.0 (Affymetrix). After staining, scanning was performed on a GeneChip Scanner 3000 (Affymetrix).

The raw microarray data was normalized using the R/Bioconductor package oligo (version 1.38.0). In brief, CEL files were read-in and subsequently normalized using the function rma. Probe sets were annotated with the affycoretools package (version 1.46.4). Entrez IDs with multiple probe sets were filtered for the probe set with the highest variance. One sample (P20 sham SVZ) was identified as an outlier and removed from further analysis. The limma package (version 3.30.7) was used for differential gene expression analysis. One set of contrast was defined to evaluate the treatment differences at both time points. P-values were adjusted for multiple testing using the Benjamini and Hochberg false discovery rate (FDR) and genes with a FDR < 0.05 were considered as significant. To compare the present data set with M1 or M2 polarization markers, we used published microarray data sets from microglia stimulated with either LPS or IL-4 (Freilich et al., 2013). The 15 most differentially expressed genes (FDR < 0.05) of microglia(LPS) and microglia(IL-4) were used to define gene sets for M1 or M2, respectively. Gene sets defined in the Kyoto Encyclopedia of Genes and Genomes (KEGG) (version dowloaded on 9. February 2017) were tested for differential enrichment using the limma function kegga. Principal component analysis and pathway-enrichment graphs were generated using R base graphics while heat maps for specified gene sets are based on the ComplexHeatmap package (version 1.12.0).

4.9. Quantitative real-time PCR validation

The microarray results were validated by quantitative real-time polymerase chain reaction (qRT-PCR) from additional SVZ samples that were not used for the microarray (n=2 for sham or HI per time point, respectively). RNA from the two samples of the same condition were pooled (500 pg per sample). Due to the low RNA amount (1 ng) per pooled sample group, we decided to validate the expression levels of microglial Igf-1. Pooled RNA was reverse-transcribed with the QuantiTect Reverse Transcription Kit (Qiagen) and qRT-PCR was performed in triplicates using Fast SYBR Green MasterMix (Roche) on a LightCycler 480 (Roche). Primers for Igf-1 and β-actin were commercially acquired (QuantiTect, Qiagen). Runs were normalized to the housekeeping gene β-actin by measuring ΔCT. The $2^{-\Delta\Delta CT}$ method was used for the calculation of the Igf-1 fold change (FC) of HI vs. sham groups per time point.

4.10. Primary neurosphere generation from SVZ tissue and microglial depletion

A third group of 18 animals was used for primary cell culture experiments. Animals underwent sham or HI surgery at P7 (n=3 sham, n=6 HI per experiment, n=3 independent experiments) and were deeply anesthetized and decapitated at P10. Rat heads were immersed in 70 % ethanol for 30 sec and kept in ice-cold HBSS until the sterile dissection. Coronal sections of 6 mm thickness of the anterior SVZ were prepared as described above. Rectangular tissue blocks including the whole ipsi- or contralateral SVZ and the adjacent medial striatum were isolated. In sham animals, all SVZ tissue blocks were pooled per experiment, whereas in HI animals, ipsi- and contralateral tissue blocks were pooled separately, resulting in 3 tissue groups: ipsilateral HI (HI ipsi), contralateral HI (HI contra), and bilateral sham tissue blocks (sham) (Fig. 16A). The pooled tissue samples were washed, dissociated with the papain neuronal dissociation kit (Miltenyi) and filtered through a 70 μm strainer. The cell

suspension was again washed and counted with trypan blue on a TC20 automated cell counter (Bio-Rad). Dissociated cells were seeded at a density of 0.3 Mio in uncoated 24-well cell culture wells (Corning). Cells were incubated in 500 µl neuronal expansion medium (DMEM/F12 1:1, Gibco; with N2 supplements [human apo-Transferrin, 100 mg / L; insulin, 25 mg / L; putrescine, 100 µM; sodium selenite, 30 nM; Sigma]; penicillin/streptomycin, 100 µg / ml, Gibco; glutaMAX, 2 mM, Gibco). The cell culture plates were incubated at 37° C in 5 % CO2. The medium was completely replaced after 2 h, followed by microglial depletion according to 3 conditions (at least 3 wells per condition per tissue group): addition of i) microglia-targeting mouse anti-CD11b saporin-conjugated antibodies (anti-CD11b SAP, 0.35 µg / ml) (Advanced Targeting Systems), ii) unspecific mouse IgG saporin-conjugated antibodies (IgG SAP, 0.35 µg / ml) (Advanced Targeting Systems) or iii) no antibodies (control) (Fig. 16A). Cell cultures were supplemented daily with recombinant human fibroblast growth factor (FGF) (20 ng / ml, R&D Systems) and recombinant human epidermal growth factor (EGF) (20 ng / ml, Peprotech). Half of the neuronal expansion medium was replaced at 3 days in culture (DIC). Neurosphere size and area were assessed after 6 DIC.

4.11. Immunocytochemistry

After 6 DIC, wells were fixed for 15 min in 4 % PFA at RT. The immunofluorescence staining (Table 1) was identical to the one described in chapter "4.5. Immunohistochemistry".

4.12. Cell culture image acquisition and analysis

Two 2.5x wide-field images per well were acquired on a Axiovert 200 microscope (Zeiss), representing 25 % of the total well surface. Number and area of neurospheres equivalent to a diameter of > 45 µm were automatically counted in ImageJ. For each experimental condition, the data from 3 wells were

averaged and extrapolated to calculate neurosphere numbers per well. For the comparison of neurosphere area distribution, the full data set was used. Qualitative 40x fluorescence images from immunohistochemically stained wells were acquired on a LSM 710 confocal microscope (Zeiss).

4.13. Flow cytometry

Dissociated samples were washed and stained with mouse anti-CD11b-FITC (1:200) (Bio-Rad) and mouse anti-CD45-PE (1:200) (Bio-Rad) in buffer solution (phosphate-buffered saline pH 7.4 [PBS], 0.5% bovine serum albumin, 2 mM Ethylene-diaminetetraacetic acid [EDTA]) at 4° C for 20 min. Samples were then washed again in buffer solution before measuring the fraction of CD11b+ CD45+ cells on an Accuri flow cytometer (BD Bioscience). All data were analyzed with FlowJo software (version 10.2).

4.14. Statistical analysis

All data sets with the exception of the microarray data (see above) were analyzed in Prism software (GraphPad, Version 6). All data are presented as mean ± standard deviation (SD) if not stated otherwise. Statistical analysis was performed with Two-way ANOVA with Tukey *post-hoc* test or One-way ANOVA with Holm-Sidak *post-hoc* test. P-values < 0.05 were considered as significant. Correlations were computed with two-tailed Pearson correlation coefficients or nonparametric Spearman correlation. Countings from ipsi- and contralateral sham hemispheres did not show significant differences, thus only ipsilateral sham data (sham) were used for statistical comparison.

5. Results

5.1. SVZ transiently enlarges while NPC density remains unaltered after HI

The Rice-Vannucci model of neonatal HI is known to result in a high variability of HI injury size (Fig. 1). Two investigators independently assessed the size of HI injury (Pearson coefficient r=0.96, 95% confidence interval [CI] 0.91-0.98, $p < 0.0001$, n=34). Based on predefined criteria, a total of 15 HI animals without histological signs of HI injury in the anterior SVZ were selected for further histological studies with a median 49 % hemispherical HI injury size (interquartile range 35 - 60%).

As previously reported (Plane et al., 2004; Ong et al., 2005; Yang and Levison 2006), HI injury induces a temporary enlargement of the SVZ and an increase in NSC / NPC proliferation (Buono et al., 2015). We measured the area of the total SVZ in sham and HI animals at 3 time points after surgery, reflecting acute, subacute and chronic stages of HI injury (Fig. 2). HI induced an early increase at P10 in SVZ size that was most prominent in the ipsilateral SVZ (0.35 [mean] ± 0.05 [SD] mm^2) as compared to the sham SVZ (0.26 ± 0.03 mm^2, $p < 0.004$). This early enlargement was transient and at P40, ipsilateral HI SVZ (0.23 ± 0.06 mm^2) adjusted to sham SVZ size (0.20 ± 0.02 mm^2). Overall, the SVZ size in both HI and sham animals markedly decreased with age.

Next, we quantified the density of proliferating PCNA+ and PAX6+ cells in the dorsolateral SVZ. Due to the vast cellular density and extensive neurogenesis in the early postnatal SVZ, we used the nuclear marker PAX6 for a most accurate cell counting. PAX6 is a transcriptional factor that is sufficient to induce a neurogenic fate in NPCs in the early postnatal SVZ (Jang and Goldman, 2011). Our results showed that the densities of PCNA+, PAX6+ or PCNA+ PAX6+ cells were not markedly different between HI and sham SVZ at any time point (Fig. 3). These results are in line with previous findings of unaltered densities of proliferating cells after ischemic stroke (Chapman et al., 2015).

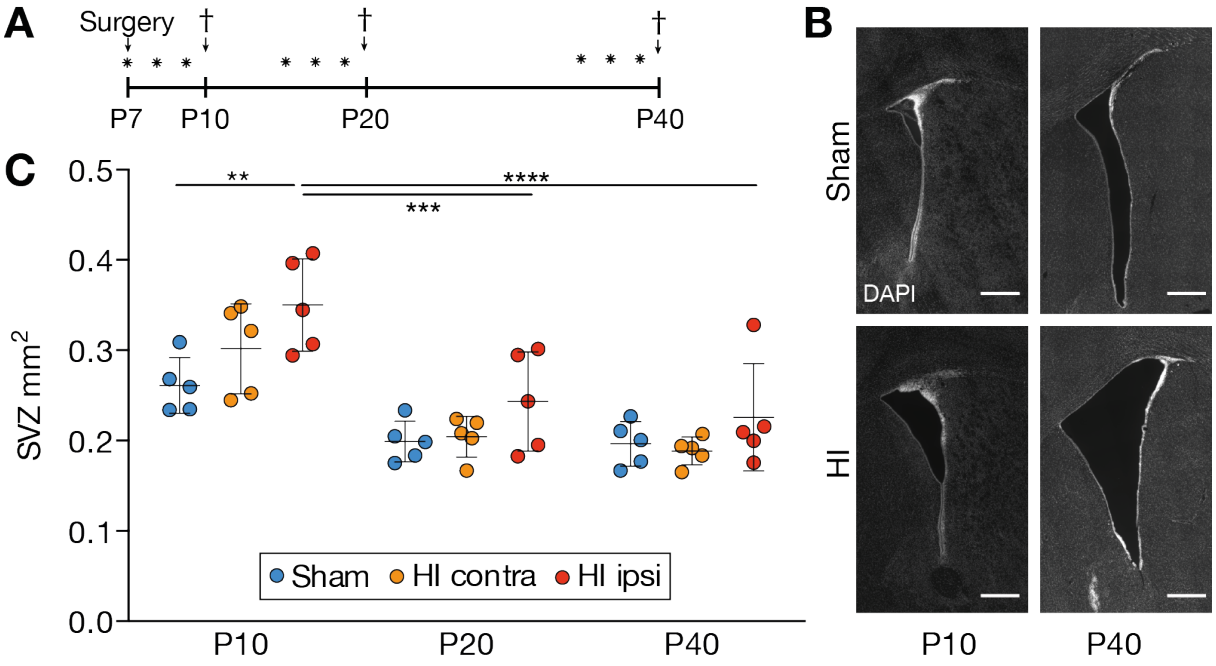

Figure 2: The SVZ temporarily expanded in size after neonatal HI. (A) Experimental timeline for the *in vivo* studies. Animals were subjected to sham or HI surgery at P7 and sacrificed at P10, P20 or P40. BrdU was injected for 3 consecutive days before sacrifice (asterisk). (B) Representative images of the ipsilateral SVZ after sham and HI surgery at P10 and P40, respectively. (C) Quantification of the SVZ size after sham and HI surgery. Mean with SD (error bars), n=5 animals, Two-way ANOVA with Tukey *post-hoc* test, ** $p < 0.01$, *** $p < 0.001$, **** $p < 0.0001$. Scale bar for (B): 500 μm.

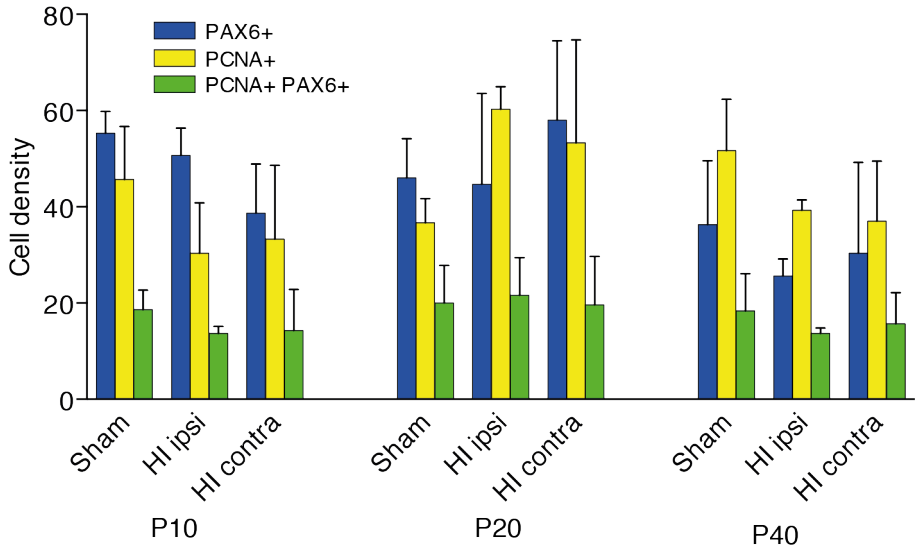

Figure 3: HI did not affect the density of cells with neurogenic fate (PAX6) and proliferating cells (PCNA) in the SVZ. PAX6+ and PCNA+ cells were counted in a 50 μm square with 10 μm depth in the median dorsolateral SVZ. Mean with SD (error bars), n=3 animals.

5.2. SVZ microglia specifically accumulate and remain activated after HI

After ischemic stroke in the adult rat, ipsilateral SVZ microglia become activated and accumulate over weeks (Thored et al., 2009). Early postnatal microglia are yet not fully maturated (Matcovitch-Natan et al., 2016; Bennett et al., 2016) and are endogenously activated in the SVZ (Shigemoto-Mogami et al., 2014), which may affect their reaction to HI injury. We therefore analyzed the impact of HI injury on SVZ microglia by quantifying microglial density (Iba1+ cells per SVZ area) and the proportion of microglial activation (number of CD68+ Iba1+ cells per total number of Iba1+ cells) (Fig. 4).

In the ipsilateral HI SVZ, the microglial density significantly increased at P10 after HI as compared to the sham SVZ (ipsilateral HI SVZ, 911 ± 57 vs. sham SVZ, 519 ± 67 Iba1+ / mm^2, $p < 0.0001$). This accumulation was maintained until P40 (1041 ± 200 vs. 590 ± 66 $p < 0.0001$) (Fig. 4C). Likewise, HI strikingly increased the proportion of activated microglia at P10 in the ipsilateral HI SVZ when compared to the sham SVZ (0.53 ± 0.13 vs. 0.25 ± 0.07 CD68+ Iba1+ / Iba1+, $p <0.0001$). This increase in activation was significantly different until P20 (0.26 ± 0.06 vs. 0.06 ± 0.03, $p<0.006$). With aging, the activation tremendously decreased in both ipsilateral HI SVZ (P10 0.53 ± 0.13 vs. P40 0.08 ± 0.03, $p < 0.0001$) and sham SVZ (0.25 ± 0.07 vs. 0.02 ± 0.02, $p \leq 0.001$) (Fig. 4D). Thus, the ipsilateral SVZ microglia responded to HI injury with early accumulation and prolonged activation. Interestingly, the contralateral SVZ responded similarly, although to a lesser extent.

Next, we investigated if these findings were specific to the SVZ or also occured in other brain regions (Fig. 4A). We therefore performed equivalent measurements in the adjacent CX and CC. In the CX, the microglial density remained unchanged between HI and sham animals from P10 (ipsilateral HI CX, 299 ± 47 vs. sham CX, 310 ± 49 Iba1+ / mm^2) until P40 (297 ± 28 vs. 266 ± 6) (Fig. 4C). In the CC, the microglial density significantly increased in the HI as compared to the sham group at P10 (HI CC, 989 ± 238 vs. sham CC, 490 ± 49, $p<0.0001$) whereas they reduced to equal densities in the HI versus sham group until P40 (367 ± 31 vs. 328 ± 32) (Fig. 4C).

HI increased the proportion of activated microglia in the CX (ipsilateral HI CX, 0.1 ± 0.12 vs. sham CX, 0.003 ± 0.004 CD68+ Iba1+ / Iba1+, $p<0.003$) and the CC (HI CC, 0.75 ± 0.13 vs. sham CC, 0.5 ± 0.17, $p<0.01$) at P10 before it drastically reduced in both HI and sham animals (Fig. 4D). Altogether, microglia in brain regions close to the SVZ were shortly activated after HI, but more importantly, did not demonstrate microglial accumulation and prolonged activation, as observed in the SVZ.

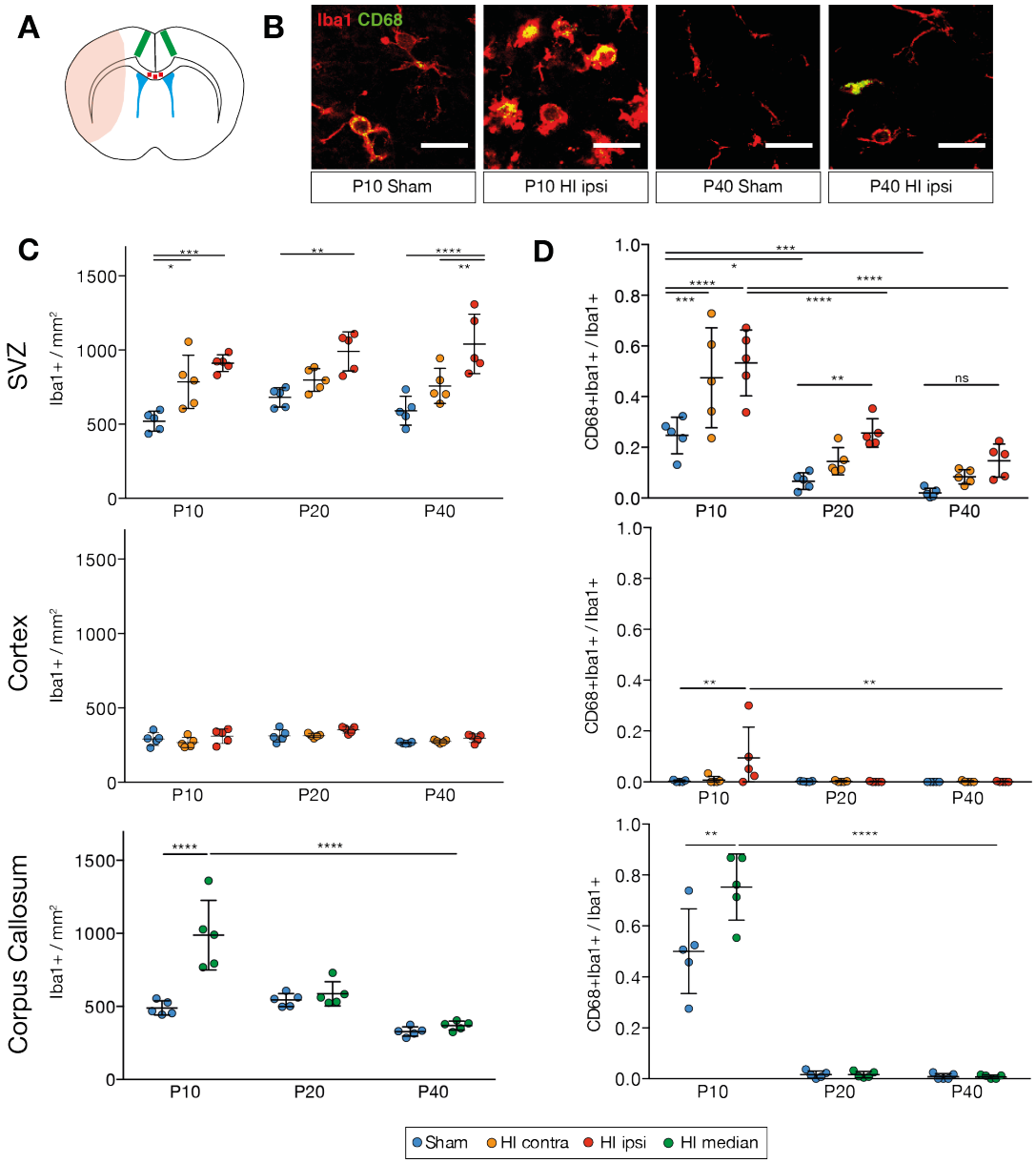

Figure 4: Microglia specifically accumulated in the SVZ and displayed prolonged activation after HI. (A) Diagram of the analyzed regions in the HI-affected (pale red) forebrain, including the SVZ (blue), the M2 supplementary motor CX (green) and the median CC (red). (B) Representative images of activated (CD68+) microglia (Iba1+) in the dorsolateral SVZ. (C) Quantification of the microglial density in different brain regions. (D). Quantification of the proportion of activated microglia in different brain regions. Mean with SD (error bars), n=5 animals, Two-way ANOVA with Tukey *post-hoc* test, ns = non-significant, * $p < 0.05$, ** $p < 0.01$, *** $p < 0.001$, **** $p < 0.0001$. Scale bar for (B): 20 μm.

.5.3. SVZ microglia proliferate early after HI

Based on the above findings of microglial accumulation in the SVZ early after HI, we next investigated if this accumulation was due to early microglial proliferation. We administered BrdU for 3 consecutive days before sacrifice to identify the percentage of proliferating SVZ microglia (number of BrdU+ Iba1+ cells per total number of Iba1+) in the dorsolateral SVZ (Fig. 5). We found a constitutionally elevated microglial proliferation in sham animals at P10 as compared to P20 and P40. HI led to a significantly induced microglial proliferation in the ipsilateral SVZ as compared to sham SVZ at P10 (ipsilateral HI SVZ, 0.16 ± 0.04 vs. sham SVZ, 0.11 ± 0.01 BrdU+ Iba1+ / Iba1+, $p < 0.014$). A concurrent analysis of Ki67+ Iba1+ proliferating microglia also depicted similar results overall, but with non-significant differences between HI and sham SVZs at P10 (data not shown), suggesting that the HI-induced proliferation mainly occurred before P10.

In comparison to the SVZ, the proportion of BrdU+ Iba1+ cells in the CX was already noticeably lower at P10 and insignificant between ipsilateral HI CX and sham CX (0.06 ± 0.03 vs. 0.05 ± 0.01) (Fig. 5). BrdU+ Iba1+ cells were practically inexistent in the CX at later time points (data not shown). Hence, microglia proliferated in the early postnatal brain and especially in the SVZ. HI further increased this proliferation within the first 3 days after HI.

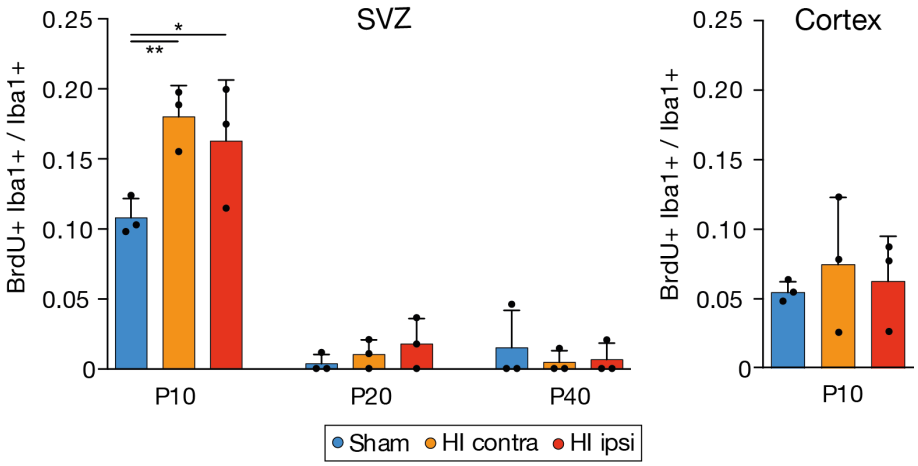

Figure 5: HI induced early proliferation of SVZ microglia. The relative proportions of proliferating (BrdU+) microglia (Iba1+) among total number of microglia were assessed in the dorsolateral SVZ and CX. Individual data shown as dots, bars as mean with SD (error bar), n=3 animals, Two-way ANOVA with Tukey *post-hoc* test, * $p < 0.05$, ** $p < 0.01$.

5.4. HI temporarily increases the proportion of amoeboid SVZ microglia

Next, we classified Iba1+ microglia in the dorsolateral SVZ upon their morphology into amoeboid, intermediate and ramified phenotypes (Fig. 6). Postnatal SVZ microglia are initially amoeboid-shaped before gradually adopting a ramified-"surveilling" morphology (Nimmerjahn et al., 2005; Shigemoto-Mogami et al., 2014). An amoeboid morphology is associated with increased activation, proliferation and phagocytosis (Kettenmann et al., 2011). To our knowledge, the morphology of early postnatal SVZ microglia has not been quantified before.

In both sham and HI, the proportion of amoeboid microglia decreased over time. Importantly, at P10, the percentage of amoeboid microglia in both ipsilateral (68.9 ± 25.2%) and contralateral HI SVZ (49.2 ± 27.6%) were strikingly increased as compared to amoeboid microglia in sham SVZ (6.8 ± 7.4%, $p \leq 0.001$). However, at P40, the percentage of amoeboid SVZ microglia became similar between HI and sham animals (ipsilateral HI, 0.9 ± 0.3 % vs. contralateral HI 1.4 ± 1.6 % vs. sham, 2.6 ± 1.1 %). In comparison, microglia in the CX remained ramified from P10 until 40 (data not shown). Thus, microglia in both ipsi- and contralateral SVZ reacted to HI with a temporary increase in amoeboid microglia.

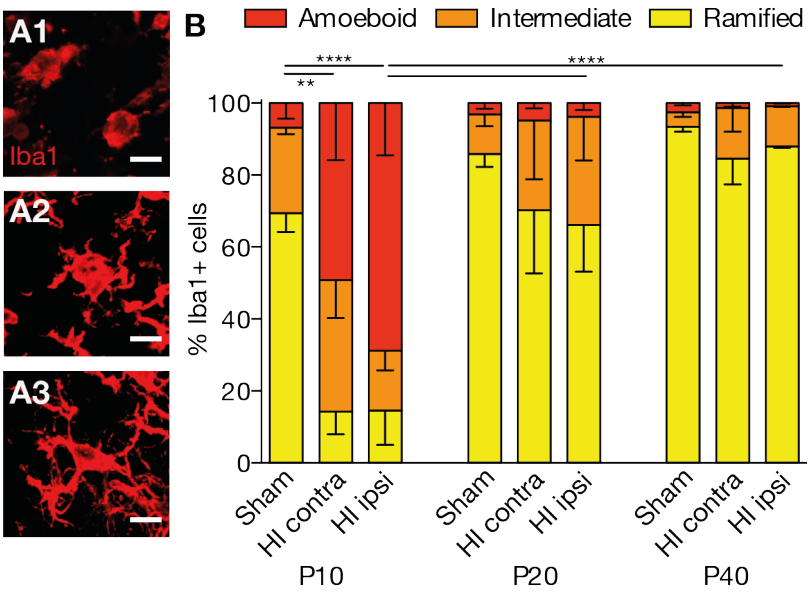

Figure 6: HI transiently increased the proportion of amoeboid SVZ microglia. (A) Microglia were classified upon their morphology into (A1) amoeboid, (A2) intermediate or (A3) ramified subtypes. (B) Proportions of Iba1+ cells in the dorsolateral SVZ according to their morphology. Mean with standard error of the mean (error bar), n=3 animals, Two-way ANOVA with Tukey *post-hoc* test, ** $p < 0.01$, **** $p < 0.001$. Scale bar for (A): 10 μm.

5.5. Increased number of ball-and-chain phagocytic SVZ microglia after HI

Phagocytosis is a key feature of microglia by which they regulate NPC numbers in the developing brain (Cunningham et al., 2013) and maintain tissue homeostasis in the adult neurogenic niches (Sierra et al., 2010; Fourgeaud et al., 2016). We next assessed microglial ball-and-chain type phagocytosis (Fig. 7A) (Sierra et al., 2010) in the dorsolateral SVZ (number of Iba1+ ball-and-chain phagocytic buds per total number of Iba1+ cells) (Fig. 7).

In sham SVZ, ball-and-chain phagocytic buds among Iba1+ cells were most prominent at P10 and continuously decreased afterwards (P10, 0.52 ± 0.1 vs. P40, 0.01 ± 0.1, $p \leq 0.0002$) (Fig 7B). In contrast, the relative number of ball-and-chain phagocytic buds increased in HI animals from P10 to P40 (ipsilateral HI SVZ, 0.06 ± 0.06 vs. 0.38 ± 0.15, $p < 0.003$), thus there was a significant difference at P40 between HI and sham ball-and-chain phagocytosis ($p < 0.009$). Importantly, ball-and-chain phagocytosis is best recognized in ramified microglia, which are considerably low in the HI SVZ at P10, though non-ramified

microglia are highly phagocytic (Kettenmann et al., 2011). Therefore, ball-and-chain defined phagocytosis likely underestimated the actual phagocytic activity of HI microglia at P10. Nevertheless, at P40, where the majority of Iba1+ cells in both HI and sham SVZ were ramified, ball-and-chain phagocytosis occurred more often in the HI SVZ as compared to the sham SVZ.

In contrast to the SVZ, microglial phagocytic activity in the CX was scarce at P10 (Fig. 7B) and undetectable afterwards (data not shown).

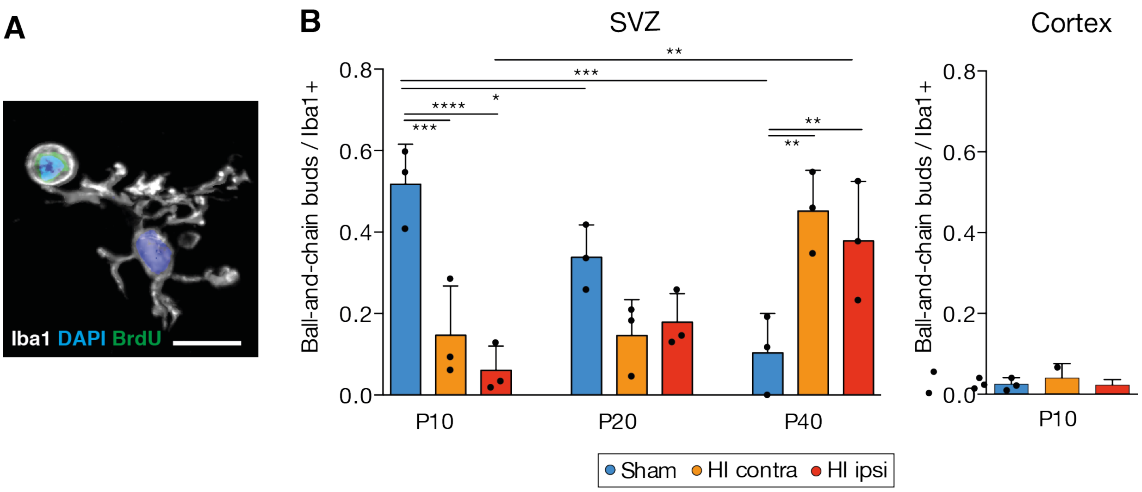

Figure 7: SVZ microglia remained phagocytic after HI at P40. (A) A representative image of a microglia engulfing a pyknotic BrdU+ cell via ball-and-chain phagocytosis. (B) Microglial phagocytosis was assessed by the frequency of ball-and-chain phagocytic buds among Iba1+ cells in the dorsolateral SVZ and the CX. Individual data shown as dots, bars as mean with SD (error bar), n=3 animals, Two-way ANOVA with Tukey *post-hoc* test, * $p < 0.05$, ** $p < 0.01$, *** $p < 0.001$, **** $p < 0.0001$. Scale bar for (A): 10 μm.

Approximately half of the ball-and-chain phagocytosed cells were BrdU+ (Fig. 7A, fig. 8), indicating that they had lately been proliferating. In rare instances, phagocytosed cells stained for the apoptosis marker CC3, but they remained systematically negative for NSC / NPC markers (sex determining region Y-box 2 [SOX2], DCX, PAX6, polysialylated-neural cell adhesion molecule [PSA-NCAM], data not shown).

In conclusion, microglial phagocytosis was eminent in the early postnatal SVZ and seemed to be preserved until P40 following HI.

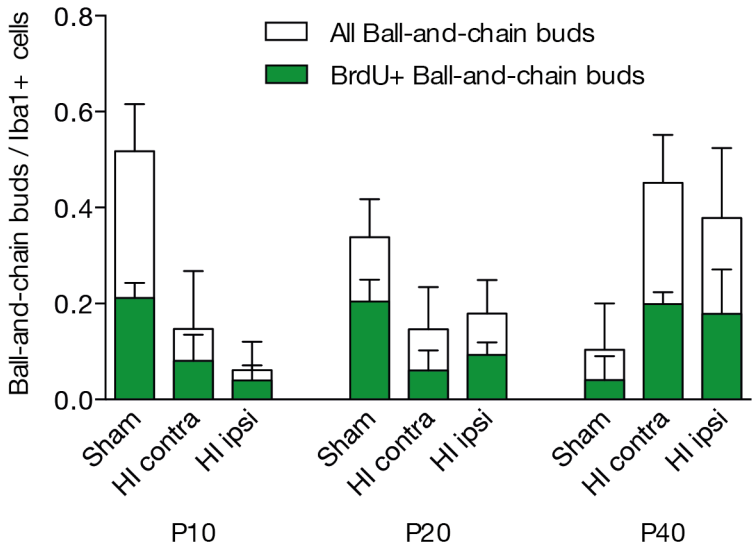

Figure 8: A considerable number of ball-and-chain phagocytosed nuclei were BrdU+. The graph shows the frequency of phagocytic buds containing BrdU+ nuclei (green bar) among the total phagocytic buds (white bar, from Fig. 7) in the dorsolateral SVZ. Mean with SD (error bar), n=3 animals.

5.6. SVZ microglia upregulate pro- and anti-inflammatory and neurotrophic genes after HI

We next analyzed the transcriptome of SVZ microglia from sham or HI animals at P10 and P20. The dorsolateral SVZ from the ipsilateral HI or ipsi- and contralateral sham hemisphere was microdissected and CD11b+ microglia isolated with magnetic bead sorting. Flow cytometry analysis demonstrated a purity of > 95 % CD11b+ CD45+ cells after sorting (Fig. 9). Total RNA was extracted from the isolated cells (RIN ≥ 8.4 [mean 9.6]) and a total of 500 pg RNA per animal sample was used for microarray experiments.

The microarray analysis revealed high expression of microglia-specific transcripts, including C1qa, Cx3cr1, P2ry12 and Tmem119 among all samples, whereas macrophage-specific gene expression was low (Fig. 10A). The principal component analysis demonstrated a grouping of most samples from the same condition (Fig. 10B). A total of 2196 genes were significantly (FDR < 0.05) differentially expressed between HI and sham samples at P10, with 1807 genes up- and 389 genes downregulated. At P20, 9930 genes were

differentially expressed with 2642 genes up- and 7288 downregulated. Overall, the FC of the significantly differentially expressed genes between HI and sham samples were modest. At P10, 19 genes were more than two-fold upregulated and 3 genes downregulated, whereas at P20, 25 genes were more than two-fold upregulated and 0 genes downregulated.

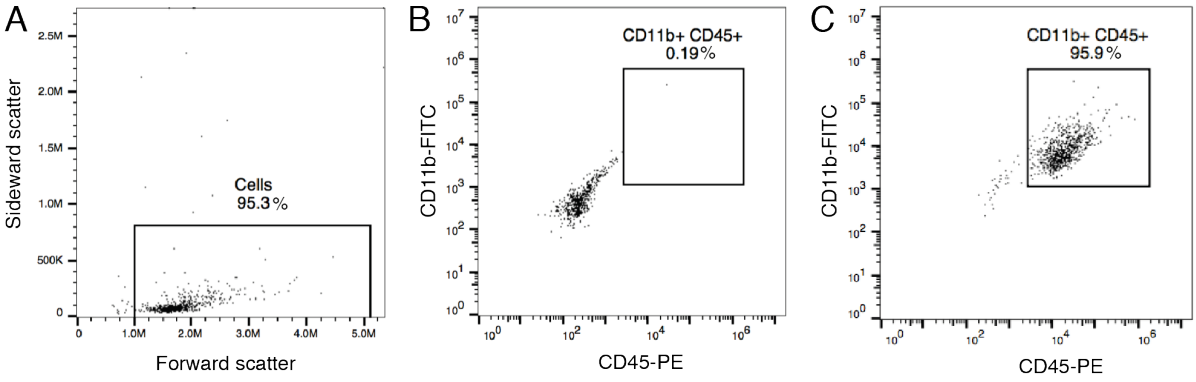

Figure 9. Magnetic bead sorting resulted in a high purity of CD11b+ CD45+ microglia. Representative data from cortical microglia isolated by CD11b+ magnetic bead sorting. (A) Gating strategy for cell identification. (B) Unstained isolated cortical cells. (C) After staining with the corresponding antibodies, isolated cortical cells were > 95% CD11b+ CD45+.

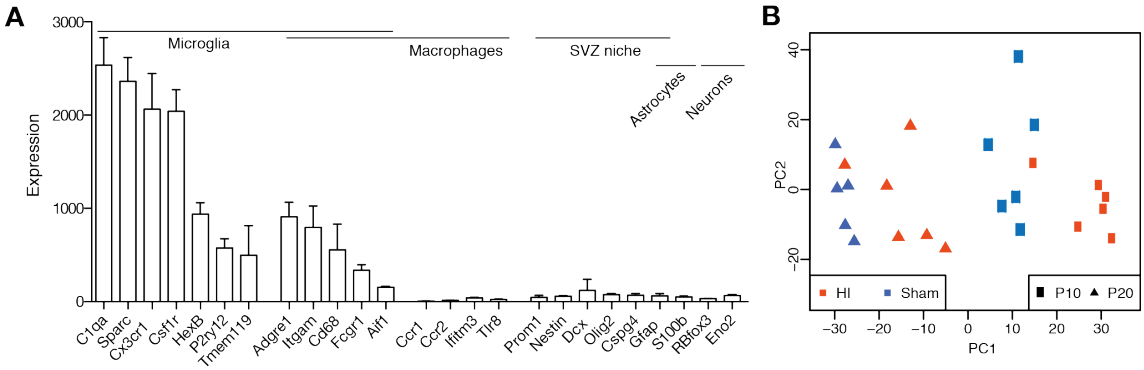

Figure 10. Enrichment of microglial transcripts in CD11b+ isolated SVZ cells. (A) Absolute expression of transcripts for microglia, macrophages, NSCs / NPCs from the SVZ niche, astrocytes or neurons among all samples. Mean with SD (error bar). (B) Principal component analysis of all samples.

The 25 most upregulated genes in ipsilateral HI SVZ microglia are listed in Table 2 for P10, and Table 3 for P20, respectively. Among those genes, we noticed a concurrent expression of both pro- and anti-inflammatory genes. Pro-inflammatory genes that were previously reported to be expressed in microglia

or macrophages included RasGef1b (Andrade et al., 2010), TNFsf9 (Yeo et al., 2012), and Rab32 (Liang et al., 2012; Haile et al., 2017) at P10, and Stat1 (Przanowski et al., 2013), Ifi27 (Uhrin et al., 2013), or Pdpn (Kerrigan et al., 2012) at P20. Vice-versa, anti-inflammatory genes were present, including Anxa2 (Zhang et al., 2015), CD206 (Casella et al., 2016), and Gpnmb (Ripoll et al., 2007; Chung et al., 2007) at P10, or Clec7 (Szulzewsky et al., 2015) and miR-146a (Saba et al., 2012) at P20. Further, P20 HI SVZ microglia differentially expressed antigen-presenting genes, including RT1-Da and RT1-Ba. At both time points, microglia upregulated genes with neurotrophic effects: Igf-1 at P10 (Ueno et al., 2013) and C3 at P20 (Rahpeymai et al., 2006).

Thus, the SVZ microglia transcriptome analysis revealed a heterogeneous pattern of upregulated genes early after HI, including concurrent expression of pro- and anti-inflammatory as well as neurotrophic genes.

The microarray data were validated by qRT-PCR of additional samples that were not previously used in the microarray. Due to the very low concentration of sample RNA, validation was performed for Igf-1, which was significantly differentially expressed at P10, but not anymore at P20. The qRT-PCR results of the additional samples were in line with the microarray data (Fig. 11).

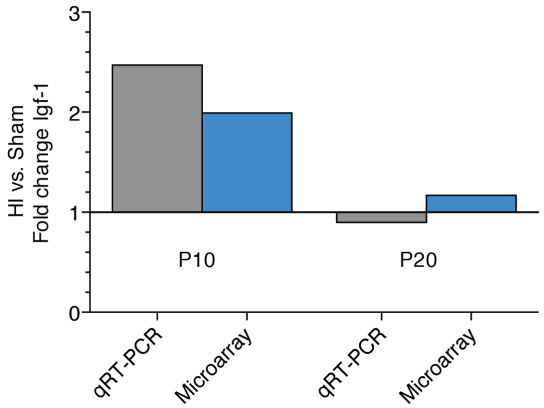

Figure 11. Validation by qRT-PCR of Igf-1 microarray measurements.

Gene symbol	Gene Name	EntrezID	FC HI vs. sham
Emb	embigin	114511	4.59
LOC100911403	membrane-spanning 4-domains subfamily A member 4A-like	100911403	4.03
Ms4a6c	membrane-spanning 4-domains, subfamily A, member 6C	690930	2.76
Anxa2	annexin A2	56611	2.74
LOC290595	hypothetical gene supported by AF152002	290595	2.73
Ms4a4a	membrane-spanning 4-domains, subfamily A, member 4A	361734	2.61
CD206	mannose receptor, C type 1	291327	2.58
Lpl	lipoprotein lipase	24539	2.48
Ccl6	chemokine (C-C motif) ligand 6	287910	2.42
Anxa5	annexin A5	25673	2.28
Sdc4	syndecan 4	24771	2.24
Stom	stomatin	296655	2.19
Rasgef1b	RasGEF domain family, member 1B	100361238	2.19
Cd8b	CD8b molecule	24931	2.18
Gpnmb	glycoprotein nmb	113955	2.09
Tnfsf9	tumor necrosis factor superfamily member 9	353218	2.09
Atp6v1e1	ATPase H+ transporting V1 subunit E1	297566	2.06
Rab32	RAB32, member RAS oncogene family	365042	2.05
Mfsd1	major facilitator superfamily domain containing 1	361957	2.01
Slirp	SRA stem-loop interacting RNA binding protein	688717	1.99
Igf-1	insulin-like growth factor 1	24482	1.99
Pygl	liver glycogen phosphorylase	64035	1.98
Igsf6	immunoglobulin superfamily, member 6	171064	1.98
Enpp6	ectonucleotide pyrophosphatase/phosphodiesterase 6	306460	1.95
Tnfaip2	TNF alpha induced protein 2	299339	1.95

Table 2: The 25 most upregulated genes in ipsilateral SVZ microglia after HI at P10 (FDR<0.05).

Gene symbol	Gene Name	EntrezID	FC HI vs. sham
LOC100910270	uncharacterized	100910270	6.37
Slfn4	schlafen 4	114247	4.51
Plac8	placenta-specific 8	360914	4.12
RT1-Da	RT1 class II, locus Da	294269	3.06
RGD1563091	similar to OEF2	500011	2.59
Clec7a	C-type lectin domain family 7, member A	502902	2.57
Rsad2	radical S-adenosyl methionine domain containing 2	65190	2.54
Clec12a	C-type lectin domain family 12, member A	680338	2.51
Ifi27	interferon, alpha-inducible protein 27	170512	2.45
Tlr1	toll-like receptor 1	305354	2.26
Pdpn	podoplanin	54320	2.18
Eif2ak2	eukaryotic translation initiation factor 2-alpha kinase 2	54287	2.17
Stat1	signal transducer and activator of transcription 1	25124	2.17
LOC102553917	putative zinc finger protein 724-like	102553917	2.16
Ifi27l2b	interferon, alpha-inducible protein 27 like 2B	299269	2.16
RT1-Ba	RT1 class II, locus Ba	309621	2.14
F10	coagulation factor X	29243	2.14
ND3	NADH dehydrogenase subunit 3	26199	2.12
LOC100911190	probable ATP-dependent RNA helicase DDX60-like	100911190	2.11
Oas1b	2-5 oligoadenylate synthetase 1B	246268	2.09
C3	complement C3	24232	2.07
LOC679827	similar to Ran-specific GTPase-activating protein	679827	2.06
Mir146a	microRNA 146a	100314241	2.06
Cxcl17	C-X-C motif chemokine ligand 17	308436	2.05
Mx2	MX dynamin like GTPase 2	286918	2.02

Table 3: The 25 most upregulated genes in ipsilateral SVZ microglia after HI at P20 (FDR<0.05).

5.7. SVZ microglia are not polarized to M1 or M2 after HI

It is proposed that microglia are polarized to either a pro-inflammatory neurotoxic M1 or anti-inflammatory neuroregenerative M2 state after acute brain injury (Hu et al., 2015). We therefore examined whether SVZ microglia express markers associated with the M1 or M2 polarization state.

We defined gene sets for commonly used M1 or M2 polarization markers (Fig. 12). Most genes from both the M1 and M2 gene sets were equally expressed among HI and sham samples at a given time point. A complementary analysis with mined microarray data (Freilich et al., 2013) from primary cultured murine microglia exposed to LPS for M1 polarization or IL-4 for M2 polarization, showed similar results (Fig. 13). Thus, our analyses do not support that SVZ microglia were polarized to M1 or M2 after neonatal HI.

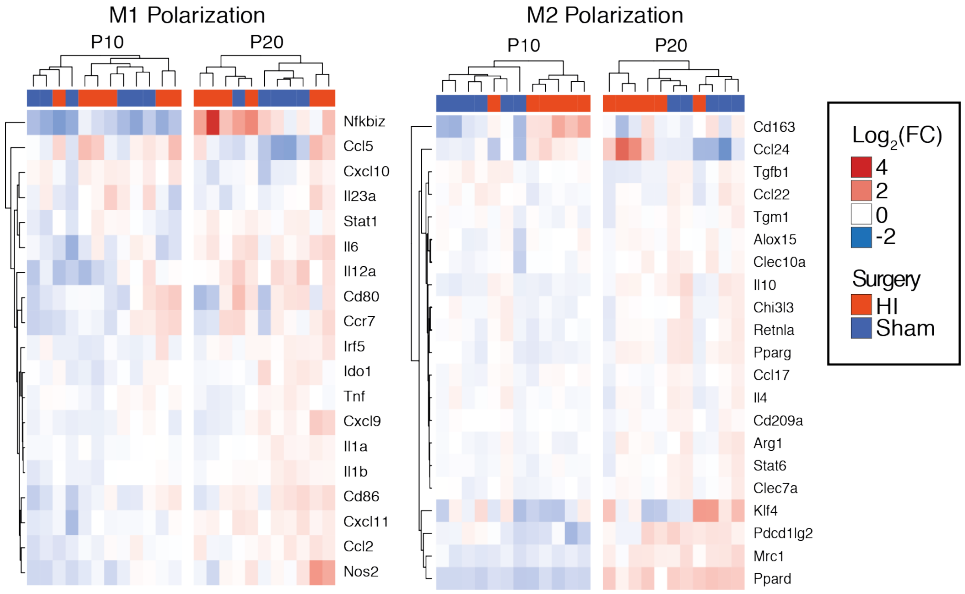

Figure 12. SVZ microglia did not adopt a M1 or M2 phenotype after neonatal HI. Heat maps showing the expression of genes commonly used as M1 or M2 polarization markers in SVZ microglia isolated from P10 and P20 sham or HI animals. Within a polarization category, most genes were equally expressed among HI and sham samples, at both time points.

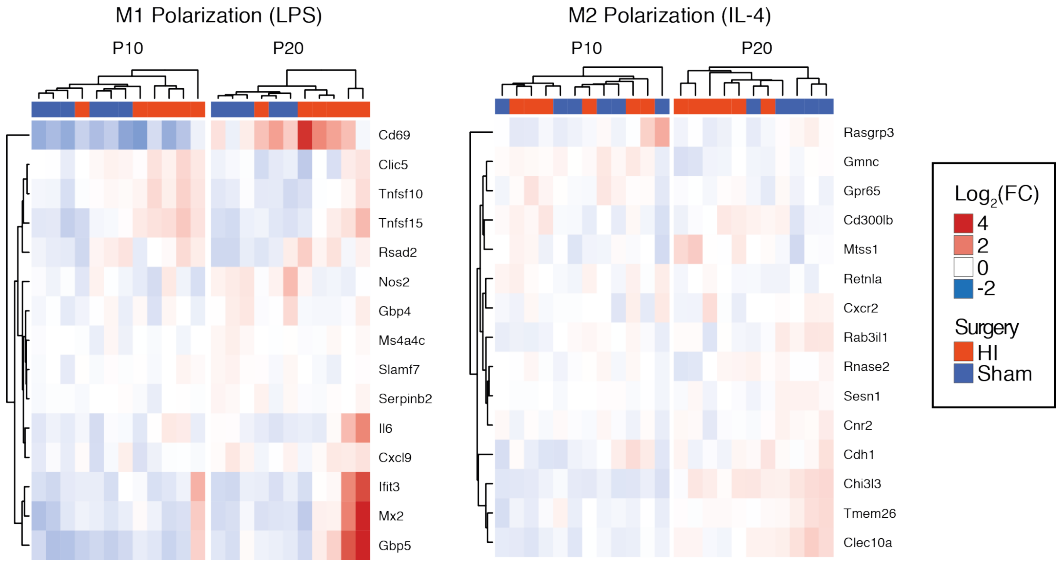

Figure 13. The SVZ microglia gene expression profile after neonatal HI did not resemble that of microglia exposed to LPS or IL-4. Heat maps for the 15 most differentially expressed genes in microglia after LPS-exposure (M1), and IL-4 exposure (M2) (from Freilich et al., 2013). As observed in Fig. 11, within one polarization category, most genes are equally expressed among HI and sham samples at P10 and P20, respectively.

5.8. SVZ microglial transcriptome is enriched for neurodegenerative pathways after HI

We performed a KEGG pathway analysis of differentially expressed genes between HI and sham SVZ microglia (Fig. 14). In HI SVZ microglia, the analysis revealed an enrichment of pathways associated with neurodegenerative diseases, including oxidative phosphorylation, ribosome, AD, Parkinson's disease, and Huntington's disease. Interestingly, these pathways were also enriched in recent microglial transcriptome studies in murine models for AD (Holtman et al., 2015) and ALS (Chiu et al., 2013). Holtman and colleagues (2015) performed a meta-analysis of these studies and identified a highly consistent consensus transcriptional profile of 295 upregulated genes, describing a generic microglial response among the different disease models which is different from a LPS-stimulated response. In this consensus gene list, we encountered multiple genes that were among the most differentially expressed genes in our data set, including Anxa2, Anxa5, Gpnmb, Mfsd1 and Igf-1 at P10, and Clec7, Rsad2, Eif2ak2, Stat1 and C3 at

P20, respectively. Interestingly, when we applied this consensus profile to our transcriptome data, we observed a considerable number of consensus genes differentially upregulated in HI SVZ microglia at P10 (Fig. 15).

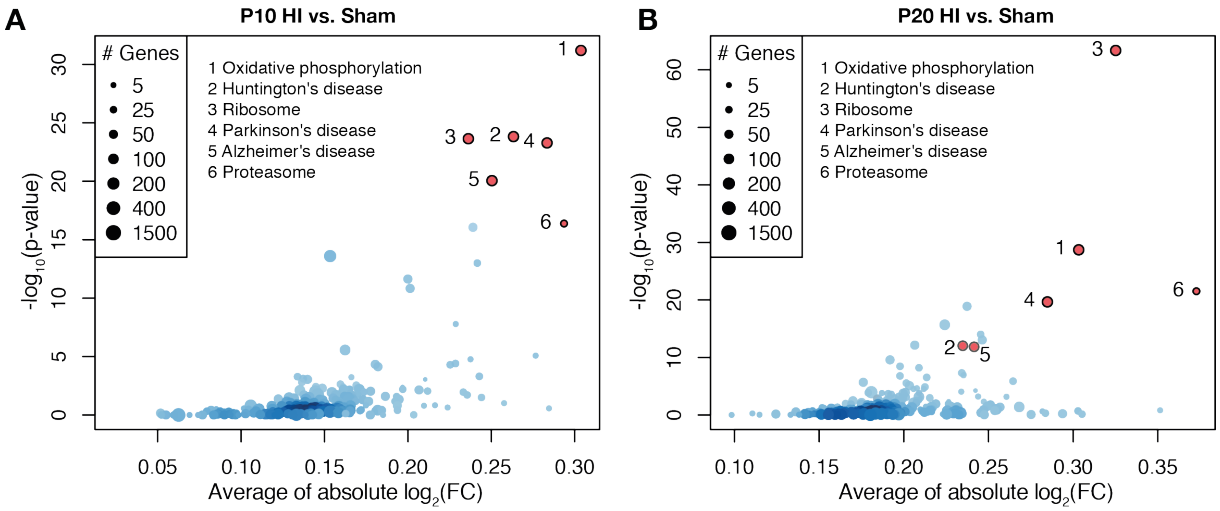

Figure 14. Pathways associated with neurodegenerative diseases were enriched in SVZ microglia after HI at P10. KEGG-pathway analysis of differentially expressed SVZ microglial genes after HI for (A) P10 and (B) P20, respectively. Pathways that were most significantly enriched at P10, are highlighted in red.

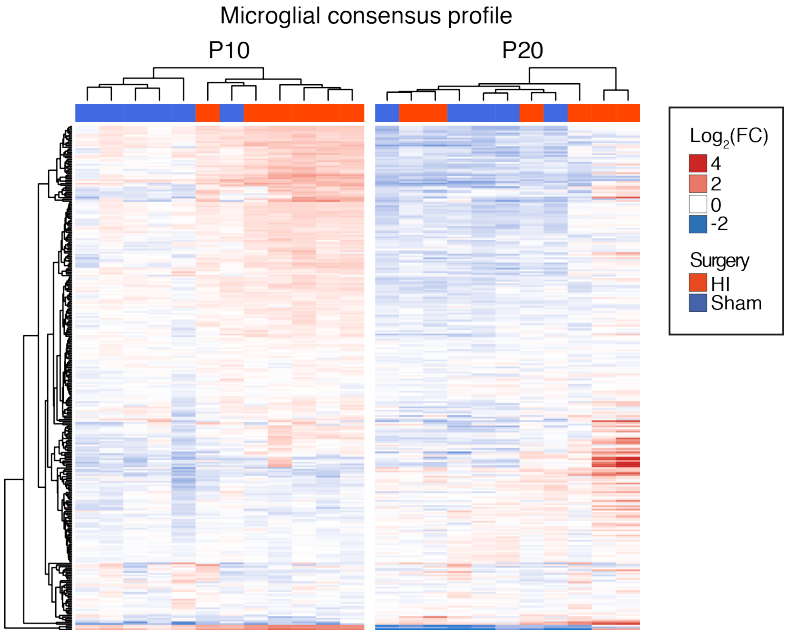

Figure. 15. The gene expression profile of SVZ microglia after neonatal HI shared similarities with that of microglia from rodent models of neurodegenerative diseases. Heat map for a consensus profile of a generic microglial response in the context of neurodegenerative diseases (from Holtman et al., 2015). A considerable number of consensus genes were upregulated in HI SVZ microglia at P10.

5.9. Microglial depletion reduces neurosphere formation

HI injury transiently induces the proliferation of NSC / NPC in the SVZ, which can be recapitulated in an *in vitro* neurosphere assay: neurospheres derived from the SVZ after HI are in higher numbers than those derived from sham SVZ (Buono et al., 2015). By using this *in vitro* model and conditional microglial depletion, we explored if the HI-induced effects on SVZ microglia had any consequences on neurosphere formation. We focused on the P10 time point where the HI-mediated effects on SVZ microglia were most striking.

Briefly, ipsi- and contralateral coronal tissue blocks that included the entire SVZ and medial striatum from P10 HI and sham animals were dissected and pooled in 3 groups: i) HI ipsi, ii) HI contra and iii) sham tissue blocks. The tissue blocks were dissociated to a single cell suspension and cultured for 6 days for neurosphere formation. After seeding, cell cultures from each tissue group were subjected to 3 culture conditions: i) control (no depletion) ii) addition of IgG SAP (unspecific cell-toxic antibody) or iii) addition of anti-CD11b SAP (CD11b+ cell-specific toxic antibody) (Fig. 16A).

After 6 DIC, neurospheres were formed that expressed nestin and DCX as NSC and NPC markers (Fig. 16B).

The proportions of CD11b+ CD45+ cells were measured by flow cytometry before seeding and after 6 DIC (Table 4). The mean percentage of CD11b+ CD45+ cells before seeding was consistently higher in HI ipsi (36%) than in HI contra (27%) or sham tissue (23%). After 6 DIC, mean CD11b+ CD45+ cell proportions were similarly decreased in control and IgG SAP conditions in sham (relative reduction from seeding proportions by 56%) or HI contra (50%) but less decreased in HI ipsi (28%). Most importantly, CD11b+ CD45+ cells were highly reduced (98%) in the anti-CD11b culture condition among all tissue groups.

To validate these results, neurosphere cultures were stained for Iba1+ after 6 DIC (Fig. 16C). In all control and IgG SAP conditions, Iba1+ cells were abundantly attached as single cells to the bottom of the well as previously noticed (Deierborg et al., 2010). Interestingly, we also detected numerous Iba1+ cells in neurospheres, a finding which to our knowledge was previously not

reported in primary neurosphere cultures. In the anti-CD11b SAP culture condition, Iba1+ cells were strikingly reduced and only few Iba1+ cells could be detected within the neurospheres. Thus, we concluded that in this culture condition, microglia were an inherent part of forming neurospheres and that their selective depletion with anti-CD11b SAP was highly effective.

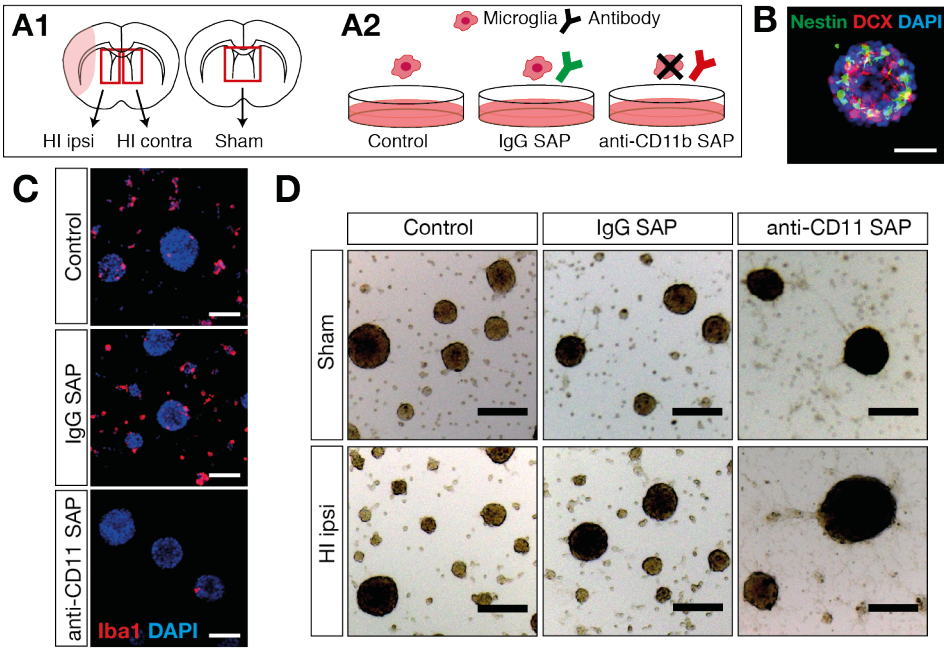

Figure 16. In vitro model to study the role of SVZ microglia in neurosphere formation. (A) Experimental design: neurosphere assay of primary cells from P10 animals with conditional depletion of microglia. (A1) Ipsi- or contralateral tissue blocks including the SVZ / medial striatum were separately isolated from HI animals, while ipsi- and contralateral tissue blocks from sham animals were pooled, resulting in 3 tissue groups (HI ipsi, HI contra and sham). (A2) The dissociated tissue blocks were exposed to 3 conditions, including no addition of antibodies (control), addition of unspecific toxic antibodies (IgG SAP), or addition of CD11b+ cell-specific toxic antibodies (anti-CD11b SAP) which target microglia. (B) Representative image of a Nestin+ DCX+ neurosphere after 6 DIC. (C) Representative images of Iba1+ cells in HI ipsi cell cultures after 6 DIC. The anti-CD11b SAP condition strikingly reduced Iba1+ cells. (C) Representative images from sham and HI ipsi cell cultures after 6 DIC. Less neurospheres were present in the anti-CD11b SAP conditions. Scale bar for (B): 50 μm, for (C): 100 μm, for (D): 200 μm.

		Before seeding CD11b+ CD45+ cells (%)			Day in culture 6 CD11b+ CD45+ cells (%)			Relative reduction of CD11b+ CD45+ cells from seeding to Day in culture 6 CD11b+ CD45+ cells (%)			
Tissue group	Condition	Experiment 1	Experiment 2	Experiment 3	Experiment 1	Experiment 2	Experiment 3	Experiment 1	Experiment 2	Experiment 3	**Average**
Sham	Control	29.0	13.7	25.0	10.5	8.1	10.1	63.8	40.9	59.6	**54.8**
	IgG SAP				18.9	4.9	6.9	34.8	64.2	72.4	**57.2**
	anti-CD11b SAP				0.2	0.2	0.4	99.3	98.5	98.4	**98.8**
HI Contra	Control	41.6	16.0	24.5	14.9	18.3	7.3	64.2	-14.4	70.2	**40.0**
	IgG SAP				15.1	8.6	7.8	63.7	46.3	68.2	**59.4**
	anti-CD11b SAP				0.5	0.3	0.6	98.8	98.1	97.6	**98.2**
HI Ipsi	Control	42.6	31.6	34.9	46.0	27.5	13.8	-8.0	13.0	60.5	**21.8**
	IgG SAP				38.8	23.3	11.2	8.9	26.3	67.9	**34.4**
	anti-CD11b SAP				0.9	1.4	0.7	97.9	95.6	98.0	**97.2**

Table 4: Percentages of CD11b+ CD45+ cells per tissue group and condition for each experiment. The relative reduction of CD11b+ CD45+ cells were similar between the control and IgG SAP condition. However, the anti-CD11b SAP condition efficiently depleted these cells. The relative reduction of CD11b+ CD45+ cells was defined as the relative difference (%) between CD11b+ CD45+ $\%_{seeding}$ and the CD11b+ CD45+ $\%_{Day\ 6}$.

Next, we quantified the number of neurospheres after 6 DIC (Fig. 16D, Fig. 17). In the control condition, the numbers of neurospheres were increased in HI ipsi compared to sham (HI ipsi, 2308 ± 363 vs. sham, 1714 ± 193 neurospheres/well, $p < 0.027$) as shown before (Buono et al., 2015). The IgG SAP condition resulted in similar numbers as the control culture condition among all tissue groups, supporting that unspecific saporin-conjugated antibodies do not impair neurosphere formation. In contrast, treatment with the anti-CD11b SAP antibody led to a significant decrease in neurosphere numbers in all tissue groups, when compared to control culture conditions ($p < 0.027$). This was most prominently observed in HI ipsi. In all anti-CD11b culture conditions the mean number of neurospheres were in a similar range (sham, 1203 ± 176 vs. HI contra, 1003 ± 204 vs. HI ipsi 924 ± 133).

We further noticed that neurospheres in the anti-CD11b condition were larger than neurospheres in the other culture conditions (Fig. 16D). The distribution of neurosphere size was similar within the same condition, independent of tissue origin (data not shown). However, the pooled anti-CD11b SAP culture conditions demonstrated an increased proportion of > 0.02 mm^2 neurospheres, when compared to the other conditions (Fig. 18).

We observed a certain variance for CD11b+ CD45+ cell proportions and neurospheres numbers among repeated experiments. We therefore correlated the percentage of CD11b+ CD45+ cells and neurosphere numbers at 6 DIC. Interestingly, we observed a positive correlation between the two factors (Spearman coefficient r=0.87, 95%CI 0.68-0.93, p <0.0001, n=27). Experiments from different tissue groups resulted in comparable neurosphere numbers if the microglial proportions were similar, thus explaining the variance in repeated experiments (Fig. 19).

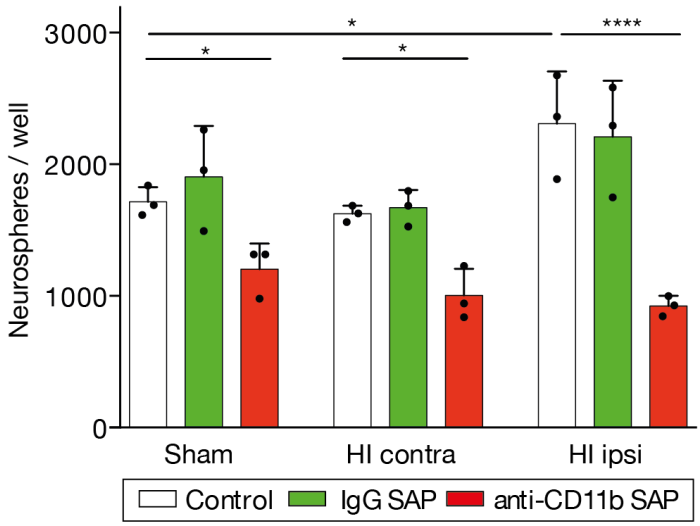

Figure 17. Microglia depletion reduced the number of neurospheres in vitro. Quantification of the number of neurospheres after 6 DIC: In the control condition, cell cultures from HI ipsi-derived tissue produced more neurospheres than sham-derived, thus reflecting HI-induced neurogenesis. Control and IgG SAP conditions showed similar results, indicating that the unspecific saporin-conjugated antibodies did not interfere with overall cell growth. Most importantly, the exposure to anti-CD11b SAP antibodies significantly decreased neurosphere numbers in all tissue groups. Individual data shown as dots, bars as mean with SD (error bar), n=3 independent experiments, One-way ANOVA with Holm-Sidak *post-hoc* test, * $p < 0.05$, **** $p < 0.0001$.

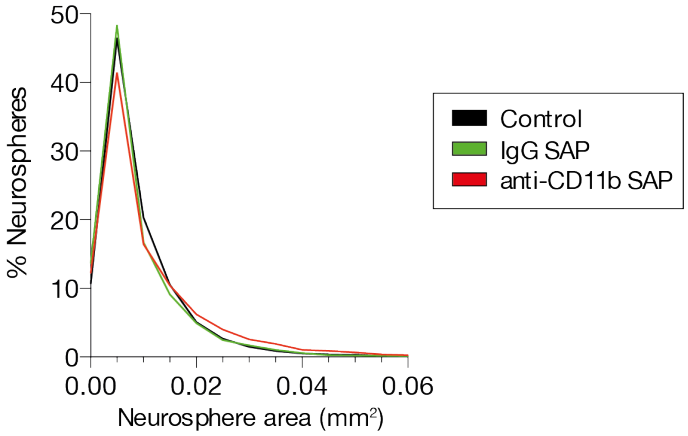

Figure 18. Microglia depletion increased the proportion of very large neurospheres *in vitro*. Tissue groups treated with the same condition did not show differences in the distribution of neurosphere area at 6 DIC and were therefore pooled. While control and IgG SAP conditions resulted in similar distribution of neurosphere area, anti-CD11b SAP exposure increased the proportion of > 0.02 mm^2 neurospheres.

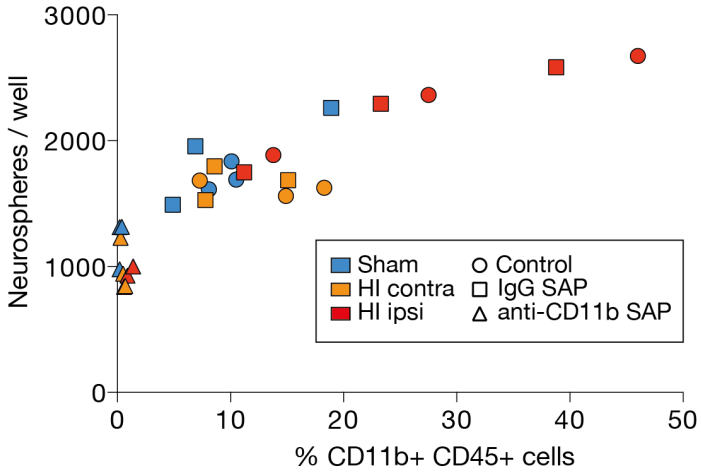

Figure 19. Positive correlation between microglial proportion and the number of neurospheres *in vitro*. The number of neurospheres increased with a higher percentage of CD11b+ CD45+ cells at 6 DIC, the highest values being observed in HI ipsi-derived cell cultures.

Overall, the cell culture experiments indicated that early postnatal CD11b+ CD45+ microglia supported neurosphere generation *in vitro* in a concentration-dependent manner. Culturing HI ipsi-derived tissue resulted in a higher number of neurospheres than sham-derived, reflecting HI-induced neurogenesis. Strikingly, depletion of microglia completely neutralized this difference and increased the proportion of very large neurospheres. Publication:

The data presented will be submitted for publication:

Fisch U, Brégère C, Geier F, Chicha L, Guzman R. Characterization of rat subventricular zone microglia after neonatal hypoxia-ischemia. Manuscript in preparation, submission scheduled for June 2016.

6. Discussion

Accumulating evidence indicates that microglia in the neurogenic niches modulate NSC / NPC proliferation and differentiation (Sato, 2015) and are therefore a potential therapeutical target. Early postnatal SVZ microglia are not yet fully maturated (Matcovitch-Natan et al., 2016; Bennett et al., 2016) and are endogenously activated (Shigemoto-Mogami et al., 2014), which might affect their response to HI injury. To date however, most research on neonatal HI focused on the perilesional microglia but not on microglia in the SVZ. We therefore aimed to investigate the impact of neonatal HI on early postnatal SVZ microglia.

6.1. Sustained accumulation and prolonged activation of SVZ microglia after HI

Our analysis on SVZ microglia indicated a sustained accumulation and prolonged activation after HI in the ipsilateral SVZ and, to a lesser extent, in the contralateral SVZ. The microglial accumulation occurred within 3 days after HI and was maintained until P40 in both ipsi- and contralateral SVZ. The proportion of activated microglia, defined by their expression of CD68 (Shigemoto-Mogami et al., 2014), was significantly increased until P20 in the ipsilateral SVZ and returned to sham levels at P40. In the adjacent CX and CC, HI affected microglial density and activation only at P10, but not afterwards. Thus, the long-lasting SVZ microglial response to HI was unique and region-specific.

In a previous study, Thored and colleagues (2009) investigated the SVZ microglial response upon ischemic stroke in the adult rat. Their results showed a microglial accumulation and activation in the ipsilateral SVZ over 16 weeks with a peak at 6 weeks after the stroke onset.

There are two noteworthy differences between our study and that by Thored and colleagues. First, the temporal dynamics were different with a rapid

neonatal SVZ microglial activation to HI, which resolved within one month and in contrast, an adult SVZ microglial reaction that remained for more than 4 months. Secondly, HI injury led to a reaction of SVZ microglia in the ipsilateral SVZ, and less extensively, also the contralateral SVZ, whereas after adult ischemic stroke, the contralateral SVZ microglia remained unaffected (Thored et al., 2009).

Several aspects may account for the observed differences between the two studies, including age, rat strains, sex distribution, cell counting methodology, as well as pathogenesis and severity of the injury. Notably, while a 2 h MCAO in the adult rat led to ipsilateral SVZ microglial accumulation (Thored et al., 2009), 30 min MCAO did not (Chapman et al., 2015), suggesting that stroke severity influences not only the neurogenic (Thored et al., 2006), but also the SVZ microglial response in the adult. On the other hand, we did not find a clear correlation between injury size and SVZ microglial accumulation or activation in the neonatal HI model (data not shown). Further, Thored et al. (2009) reported total microglial numbers, while we reported microglial density, which takes into account changes in SVZ size. However, we propose that the age difference, reflecting different microglial developmental stages between the early postnatal and the adult animal (Matcovitch-Natan et al., 2016, Bennett et al., 2016), is especially important. Interestingly, our results indicated that the SVZ microglial reaction was not limited to the ipsilateral, but also involved the contralateral SVZ, although to a lesser degree. Early postnatal microglia resemble rather an embryological stage before adopting an adult phenotype (Matcovitch-Natan et al., 2016, Bennett et al., 2016) and react more extensively, than their adult counterparts when directly stimulated (Denker et al., 2007; Christensen et al., 2014). It may be possible that the endogenous activation of SVZ microglia during that time period (Shigemoto-Mogami et al., 2014) render them exceptionally sensitive to remote tissue damage. Importantly, our histological analyses did not suggest that such a potential increased sensitivity would permanently affect the SVZ microglia. On the contrary, the fact that their response upon HI injury appeared to resolve faster than what was observed after adult ischemic stroke, suggests that either intrinsic or extrinsic factors in early postnatal SVZ microglia favour a recovery.

6.2. Early SVZ microglial proliferation is increased by HI

BrdU-labelling in the dorsolateral sham SVZ indicated a noticeable microglial proliferation at P10 but not afterwards. Neonatal HI injury potentiated this proliferation in both the ipsi- and contralateral SVZ at P10, but did not induce proliferation thereafter. However, our results did not indicate if this early microglial proliferation was sufficient for the long-standing cell accumulation or if it was partially caused by additional migrating microglia / macrophages. The latter possibility remains unanswered, as current IHC techniques cannot specifically differentiate rat microglia from macrophages. It was previously proposed that periventricular microglia in the early postnatal brain are mainly derived from migrating macrophages (Ling and Wong, 1993), and it is conceivable that monocytes transmigrate to the brain after HI via the highly vascularized SVZ. On the other hand, CD11b+ cells isolated from the SVZ at P10 and P20 highly expressed typical microglial genes, thus a significant contribution of macrophages is therefore less likely.

6.3. SVZ microglia remain phagocytic after HI

Microglial phagocytosis is fundamental for CNS development and maintenance, immune defense, and tissue repair (Sierra et al., 2013; Neumann et al., 2009). SVZ microglia regulate the number of cortical neurons by phagocytosing NPCs during embryogenesis (Cunningham et al., 2013). Postnatally, microglia maintain tissue homeostasis by phagocytosing apoptotic NPCs in the SVZ and the SGZ via ball-and-chain shaped engulfing buds (Sierra et al., 2010; Fourgeaud et al., 2016; Frost and Schafer, 2016). Early postnatal periventricular microglia are highly phagocytic (Ling and Wong, 1993; Hristova et al., 2010) and gradually change from an amoeboid to a ramified morphology.

In this study, we assessed the morphology and the number of ball-and-chain phagocytic buds in relation to microglial numbers in the dorsolateral SVZ. In sham animals, the proportion of amoeboid microglia decreased continuously with age. However, HI injury temporarily increased the proportion of amoeboid microglia in both ipsi- and contralateral SVZ at P10.

While the relative number of ball-and-chain phagocytic buds continuously decreased among sham SVZ microglia, it contrariwise increased in HI animals. These results have important limitations. Ball-and-chain phagocytic buds are best observed in ramified microglia which must be considered when interpreting the countings in P10 HI SVZ microglia where only a minority of cells were ramified. Further, few studies have so far quantified microglial phagocytosis *in vivo* (Sierra et al., 2013) and ball-and-chain buds may represent only one of several forms of microglial phagocytosis. Microglial phagocytosis is a fast process and completed in less than 30 min (Morsch et al., 2015). Thus, our results from fixed tissue represented a snapshot and could only approximate phagocytic activity *in vivo.* Despite these limitations, our data clearly indicated marked differences in ball-and-chain-type phagocytosis between HI and sham SVZ microglia at P40 when both HI and sham SVZ microglia were ramified.

In this study, phagocytosed cells very rarely stained for the apoptotic marker CC3. As it is suggested that microglia can also phagocytose live cells (Brown and Neher, 2014), it is conceivable that SVZ microglia preferentially phagocytose live NSCs / NPCs. It is noteworthy that, roughly half of the engulfed cells were BrdU+, indicating that they were proliferating within 3 days before sacrifice. However, the engulfed cells did not stain for NSC / NPC markers, including SOX2, PAX6, PSA-NCAM and DCX. Thus the identity of these cells remained unknown. In a previous study in the adult hippocampus, cells engulfed by microglia stained positively for PSA-NCAM, but not DCX. A different degradation rate of those proteins was suggested to be responsible for this discrepancy (Sierra et al., 2010). Similarly, in the early postnatal SVZ, a rapid protein degradation by microglia could be a potential reason for the systematic negative stainings for NSC / NPC markers.

6.4. SVZ microglia express neurotrophic and immunomodulatory genes early after HI

We performed a microarray transcriptome analysis of purified CD11b+ SVZ microglia from individual sham and HI animals. The results indicated a high enrichment of microglial, but not macrophage-specific genes. Of note, we also noticed an elevated gene expression of NSC / NPC markers, such as Dcx. Flow cytometry analysis indicated a > 95 % purity of CD11b+ isolated cells and therefore it is possible that NSC / NPC transcripts originated from the 5 % CD11b- cells. Another potential explanation comes from a study by Solga and colleagues (2015). These authors found neuronal and oligodendroglial transcripts, but not proteins, in brainstem microglia and hypothesized that the presence of these mRNAs may reflect microglial RNA uptake from their surroundings. Likewise, NSC / NPC transcripts in SVZ microglia might also reflect an analog RNA uptake.

HI induced both pro- and anti-inflammatory genes, illustrating the complexity of the SVZ microglial reaction. Of note, IL-1β, IL-6, TNF-α and IFN-γ, which are strongly upregulated in acute inflammation (Monje et al., 2003; Butovsky et al., 2006, Cacci et al., 2008) were not differently expressed between HI and sham SVZ microglia (data not shown), underscoring that the SVZ microglia were not directly affected by the HI injury.

Among the 25 most upregulated genes in P10 ipsilateral SVZ microglia, we noted IGF-1 and Gpnmb. IGF-1 is a well-known neurotrophic factor that can affect NPCs in multiple ways, including anti-apoptotic effects (Chrysis et al., 2012), reduction of cell cycle length and increase of cell cycle reentry (Hodge et al., 2004). SVZ and striatal microglia upregulate IGF-1 after ischemic stroke in the rat (Thored et al., 2009; Chapman et al., 2015). Microglial IGF-1 production is essential for cortical neuronal survival (Ueno et al., 2013) and is neuroprotective after ischemic stroke (Lalancette-Hébert et al., 2007).

In the rodent brain, Gpnmb is predominantly expressed by microglia (Huang et al., 2012). It is found to be upregulated by microglia after systemic LPS exposure (Huang et al., 2012), in a model of AD (Kamphuis et al., 2016), and in the context of glioma (Szulzewsky et al., 2015). The perilesional brain

tissue after ischemia and the retina after optic nerve transection also demonstrate an increased expression of Gpnmb (Buga et al., 2012; Nakano et al., 2014, Yasuda et al., 2016). In murine macrophages, Gpnmb attenuates the inflammatory response upon LPS or IFN-γ stimulation (Ripoll et al., 2007) and negatively regulates T-cell activation (Chung et al., 2007). Furthermore, Gpnmb is associated with neuroprotective effects in murine models for brain ischemia (Nakano et al., 2014) and ALS (Tanaka et al., 2012). Thus, the SVZ microglia transcriptome reflects a heterogeneous response to neonatal HI with neurotrophic Igf-1 and immunomodulatory Gpnmb among the most upregulated genes at P10.

6.5. SVZ microglia do not adopt a M1 or M2 polarization after HI

The concept of microglial polarization originated from *in vitro* observations in macrophages. Upon activation, microglia are thought to adopt a pro-inflammatory neurotoxic M1 or anti-inflammatory neuroregenerative M2 state (Hu et al., 2015). Although this concept is widely used for microglial phenotype characterization, recent *in vivo* transcriptome studies demonstrate that activated microglia / macrophages simultaneously co-express M1 / M2 polarization genes rather than displaying a relevant tendency toward either a M1 or M2 phenotype (Chiu et al., 2013; Holtman et al., 2015; Szulzewsky et al., 2015; Morganti et al., 2016; Kim et al., 2016; Ransohoff, 2016). We explored if SVZ microglia adopt a M1 or M2 state after HI injury with two independent gene sets from commonly used polarization markers an from an *in vitro* polarized microglial transcriptome analysis (Freilich et al., 2013). Overall, these analyses did not indicate a clear tendency of SVZ microglia adopting either a M1 or M2 state after HI, although individual M1 / M2 markers (e.g. CD206 for M2 at P10, Stat1 for M1 at P20) were found among the most upregulated genes. On the contrary, the data rather suggested a moderate upregulation of both M1 / M2 markers with age that was independent of HI or sham surgery.

6.6. SVZ microglia transiently upregulate neurodegeneration-associated genes after HI

The KEGG pathway analysis of differentially expressed genes in P10 HI SVZ microglia showed an enrichment of pathways that are associated with neurodegenerative diseases. Interestingly, similar pathways were enriched in isolated microglia in a transgenic ALS model. In this model, microglia concurrently upregulated neurotoxic and neurotrophic genes which were distinct from genes upregulated after LPS-exposure. Strikingly, the microglial genes which were most upregulated in the ALS model and in parallel downregulated after LPS-exposure were Igf-1 and Gpnmb (Chiu et al., 2013). These two genes are also found among the most upregulated genes in SVZ microglia after HI at P10. Igf-1 and Gpnmb were also distinctively upregulated in other microglial transcriptome studies in animal models for AD, accelerated aging, and physiological aging (Srinivasan et al., 2016, Holtman et al., 2015). Holtman and colleagues (2015) identified a gene set, including Igf-1 and Gpnmb, which was highly consistent among microglia in these animal models of neurodegenerative diseases. When applying this consensus gene set to our transcriptome data, we observed a considerable number of genes upregulated in HI SVZ microglia at P10. This was unexpected given the different pathogenesis of HI injury and neurodegenerative diseases like AD and ALS. There are multiple differences between our and the aforementioned transcriptome studies, including species, age, microglia isolation protocols and gene expression profiling methods, which can act as potential confounding factors. Nevertheless, the shared gene expression pattern is remarkable and merits further investigation. At this stage, we would like to refrain from characterizing the SVZ microglia after neonatal HI as “neurodegenerative-like”. Rather, our data show that the generic microglial response pattern observed in different neurodegenerative diseases (Holtman et al., 2015, Colonna and Butovsky, 2017) may actually be shared by radically distinct CNS pathologies.

Altogether, the gene expression induction of SVZ microglia upon HI is complex and beyond a simplified categorization into a pro- or anti-inflammatory response. The comparison with recent microglial transcriptome studies in

models of neurodegenerative diseases revealed a marked overlap of upregulated genes which potentially indicates a generic microglial response to various pathologies (Chiu et al., 2013; Holtman et al., 2015).

6.7. SVZ microglia support neurosphere generation in vitro

The HI-induced proliferation of NSCs / NPCs in the SVZ can be recapitulated in an *in vitro* neurosphere assay (Buono et al., 2015). By using this neurosphere assay and specific depletion of microglia, we explored if the HI-induced effects on SVZ microglia had any consequences on neurosphere generation. For these *in vitro* experiments, we focused on P10 SVZ microglia since the HI-mediated effects were the strongest at this time point. Our analyses showed that microglia were not only present as single cells at the bottom of the cell culture well (Deierborg et al., 2010), but also within the neurospheres. As previously reported, the number of neurospheres derived from the ipsilateral HI SVZ were significantly increased than that derived from sham SVZ (Buono et al., 2015). However, this HI-enhanced proliferation was completely neutralized when microglia were depleted. The microglial percentage and the neurosphere numbers positively correlated among all conditions, suggesting that microglia supported neurosphere formation in a concentration-dependent manner.

These findings are in line with several previous *in vitro* studies, which demonstrated microglial support of NPC and neurosphere proliferation. Conditioned medium from mixed cell cultures containing microglia from young (Walton et al., 2006) or ischemic rodent brain tissue (Deierborg et al., 2010) promoted NPC proliferation. In a co-culture system, human microglia had inhibiting effects on NPC differentiation (Liu et al., 2013). The inhibiting effects of LPS and IFN-γ on murine neurosphere formation was attenuated by the presence of microglia (Li et al., 2010, Ortega et al., 2014). Finally, IL-6, most likely derived from microglia, promoted neurosphere proliferation within the first 48 h after neonatal HI in rats (Covey et al., 2011).

In accordance with the findings by Covey and colleagues (2011), the SVZ microglia transcriptome data showed no difference in IL-6 gene expression between HI and sham animals at 3 days after the injury. Furthermore, IL-1β, TNF-α and IFN-γ, which modulate neurogenesis and oligodendrogenesis *in vitro* (Shigemoto-Mogami et al., 2014), were not differently expressed among HI and sham animals. However, early postnatal SVZ microglia highly expressed IGF-1 (Shigemoto-Mogami et al., 2014), which we found to be upregulated after HI. IGF-1 was shown to stimulate neurosphere proliferation *in vitro* (Erickson et al., 2008; Supeno et al., 2013) and neuronal survival *in vivo* (Ueno et al., 2013). Future studies are warranted to identify the SVZ microglial mediators which enhance neurosphere formation after HI.

SVZ-derived NPCs were recently shown to establish functional gap junctions with microglia (Talaveron et al., 2015). Our *in vitro* experiments showed that microglia were an integral part of neurospheres. Hence, it is conceivable that microglia may modulate NPC not only via secreted factors but also through direct cell-cell-interaction. Importantly, microglial interaction with NPCs is reciprocal with NPCs enhancing microglial proliferation (Mosher et al., 2012; Liu et al., 2013), which is underlined by our results, where microglial proportions positively correlated with neurosphere numbers with highest values in cultures from the ipsilateral HI SVZ.

7. Conclusions

Our report provides the first in depth characterization of the microglial phenotype in the rat SVZ after neonatal HI. Microglia are an inherent cellular component of the early postnatal SVZ and undergo specific developmental changes that are disrupted by neonatal HI injury. The SVZ microglial response upon HI, manifested by cellular accumulation, prolonged activation and phagocytosis, is SVZ-specific and does not occur in adjacent brain regions. Nevertheless, the SVZ microglial response is not permanent and resolves faster than what is observed in rodent models of adult stroke. SVZ microglia are sensitive to remote HI injury and upregulate both pro- and anti-inflammatory genes and do not adopt a M1 or M2 polarized state, but instead share to a certain degree a gene expression pattern with microglia in models of neurodegenerative diseases. *In vitro,* early postnatal microglia appear to show trophic support for neurosphere generation in a concentration dependent manner.

The microglial reaction upon imbalances in the CNS is context-dependent. Concurrent positive and negative effects on CNS regeneration makes the microglial response a complex subject to characterize. Accumulating evidence indicates that the microenvironment and the temporal dynamics of the microglial reaction are essential factors which need to be considered when characterizing the microglial phenotype after brain injury. Hence, we specifically focused our studies on microglia in the SVZ at acute, subacute and chronic stages after neonatal HI.

Our findings contribute to a better understanding of the diverse microglial roles in different CNS regions and give insight into the microglial responses upon remote brain injury. A major result of this study is that early postnatal SVZ microglia are sensitive to distant HI injury and show a prolonged subacute response when compared to their counterparts in adjacent brain regions. Such findings are potentially important when considering microglia as a therapeutic target after brain injury. Although currently unavailable (Hagberg et al., 2015), a specific pharmacological modulation of microglia upon injury will likely systemically affect microglia. It is therefore crucial to first obtain a fundamental

understanding of microglial responses in specific brain regions, including the SVZ, in order to estimate consequences of such potential treatments for the whole CNS.

Microglia in the SVZ are increasingly recognized as modulators of neurogenesis (Sato, 2015). Our descriptive *in vivo* studies did not demonstrate direct evidence that SVZ microglia are required for the HI-induced increase in SVZ neurogenesis. One possibility to further approach this question would be a selective depletion of SVZ microglia before neonatal HI. However, depletion options in the rat are limited. Reduction of SVZ microglia in the adult rat by saporin-conjugated antibodies were insufficient (Heldmann et al., 2011). While depletion of perilesional microglia via uptake of clodronate liposomes was successful in the rat neonate after MCAO (Faustino et al., 2011), its specificity in the SVZ must be carefully evaluated since SVZ NPCs also avidly engulf liposomes (Lu et al., 2011). We therefore consider a transgenic mouse model for conditional microglial depletion as more suitable to address this question. Furthermore, transgenic mouse models offer the advantage to differentiate microglia from macrophages that may play a different role in SVZ neurogenesis.

Although our *in vivo* studies did not show direct evidence for SVZ microglia significantly enhancing neurogenesis after HI, the results did not suggest a detrimental effect either. The microglial upregulation of neurotrophic and immunomodulatory genes after HI as well as the trophic support of microglia on neurosphere generation are a promising basis for further research.

8. References

Ajami B, Bennett JL, Krieger C, McNagny KM, Rossi FM. Infiltrating monocytes trigger EAE progression, but do not contribute to the resident microglia pool. Nat Neurosci. 2011;14(9):1142-9.

Ajami B, Bennett JL, Krieger C, Tetzlaff W, Rossi FM. Local self-renewal can sustain CNS microglia maintenance and function throughout adult life. Nat Neurosci. 2007;10(12):1538-43.

Alliot F, Godin I, Pessac B. Microglia derive from progenitors, originating from the yolk sac, and which proliferate in the brain. Brain Res Dev Brain Res. 1999;117(2):145-52.

Alvarez-Díaz A, Hilario E, de Cerio FG, Valls-i-Soler A, Alvarez-Díaz FJ. Hypoxic-ischemic injury in the immature brain--key vascular and cellular players. Neonatology. 2007;92(4):227-35.

Andrade WA, Silva AM, Alves VS, Salgado AP, Melo MB, Andrade HM, Dall'Orto FV, Garcia SA, Silveira TN, Gazzinelli RT. Early endosome localization and activity of RasGEF1b, a toll-like receptor-inducible Ras guanine-nucleotide exchange factor. Genes Immun. 2010;11(6):447-57.

Arandjelovic S, Ravichandran KS. Phagocytosis of apoptotic cells in homeostasis. Nat Immunol. 2015;16(9):907-17.

Arvidsson A, Collin T, Kirik D, Kokaia Z, Lindvall O. Neuronal replacement from endogenous precursors in the adult brain after stroke. Nat Med. 2002;8(9):963-70.

Battista D, Ferrari CC, Gage FH, Pitossi FJ. Neurogenic niche modulation by activated microglia: transforming growth factor beta increases neurogenesis in the adult dentate gyrus. Eur J Neurosci. 2006;23(1):83-93.

Bennett ML, Bennett FC, Liddelow SA, Ajami B, Zamanian JL, Fernhoff NB, Mulinyawe SB, Bohlen CJ, Adil A, Tucker A, Weissman IL, Chang EF, Li G, Grant GA, Hayden Gephart MG, Barres BA. New tools for studying microglia in the mouse and human CNS. Proc Natl Acad Sci U S A. 2016;113(12):E1738-46.

Billiards SS, Haynes RL, Folkerth RD, Trachtenberg FL, Liu LG, Volpe JJ, Kinney HC. Development of microglia in the cerebral white matter of the human fetus and infant. J Comp Neurol. 2006;497(2):199-208.

Bonestroo HJ, Nijboer CH, van Velthoven CT, Kavelaars A, Hack CE, van Bel F, Heijnen CJ. Cerebral and hepatic inflammatory response after neonatal hypoxia-ischemia in newborn rats. Dev Neurosci. 2013;35(2-3):197-211.

Brown GC, Neher JJ. Microglial phagocytosis of live neurons. Nat Rev Neurosci. 2014;15(4):209-16.

Bruttger J, Karram K, Wörtge S, Regen T, Marini F, Hoppmann N, Klein M, Blank T, Yona S, Wolf Y, Mack M, Pinteaux E, Müller W, Zipp F, Binder H, Bopp T, Prinz M, Jung S, Waisman A. Genetic Cell Ablation Reveals Clusters of Local Self-Renewing Microglia in the Mammalian Central Nervous System. Immunity. 2015;43(1):92-106.

Buga AM, Scholz CJ, Kumar S, Herndon JG, Alexandru D, Cojocaru GR, Dandekar T, Popa-Wagner A. Identification of new therapeutic targets by genome-wide analysis of gene expression in the ipsilateral cortex of aged rats after stroke. PLoS One. 2012;7(12):e50985.

Buono KD, Goodus MT, Guardia Clausi M, Jiang Y, Loporchio D, Levison SW. Mechanisms of mouse neural precursor expansion after neonatal hypoxia-ischemia. J Neurosci. 2015;35(23):8855-65.

Burek MJ, Oppenheim RW. Programmed cell death in the developing nervous system. Brain Pathol. 1996;6(4):427-46.

Butovsky O, Talpalar AE, Ben-Yaakov K, Schwartz M. Activation of microglia by aggregated beta-amyloid or lipopolysaccharide impairs MHC-II expression and renders them cytotoxic whereas IFN-gamma and IL-4 render them protective. Mol Cell Neurosci. 2005;29(3):381-93.

Butovsky O, Ziv Y, Schwartz A, Landa G, Talpalar AE, Pluchino S, Martino G, Schwartz M. Microglia activated by IL-4 or IFN-gamma differentially induce neurogenesis and oligodendrogenesis from adult stem/progenitor cells. Mol Cell Neurosci. 2006;31(1):149-60.

Cacci E, Ajmone-Cat MA, Anelli T, Biagioni S, Minghetti L. In vitro neuronal and glial differentiation from embryonic or adult neural precursor cells are differently affected by chronic or acute activation of microglia. Glia. 2008;56(4):412-25.

Casella G, Garzetti L, Gatta AT, Finardi A, Maiorino C, Ruffini F, Martino G, Muzio L, Furlan R. IL4 induces IL6-producing M2 macrophages associated to inhibition of neuroinflammation in vitro and in vivo. J Neuroinflammation. 2016;13(1):139.

Chapman KZ, Ge R, Monni E, Tatarishvili J, Ahlenius H, Arvidsson A, Ekdahl CT, Lindvall O, Kokaia Z. Inflammation without neuronal death triggers striatal neurogenesis comparable to stroke. Neurobiol Dis. 2015;83:1-15.

Chiu IM, Morimoto ET, Goodarzi H, Liao JT, O'Keeffe S, Phatnani HP, Muratet M, Carroll MC, Levy S, Tavazoie S, Myers RM, Maniatis T. A neurodegeneration-specific gene-expression signature of acutely isolated microglia from an amyotrophic lateral sclerosis mouse model. Cell Rep. 2013;4(2):385-401.

Choi YS, Cho HY, Hoyt KR, Naegele JR, Obrietan K. IGF-1 receptor-mediated ERK/MAPK signaling couples status epilepticus to progenitor cell proliferation in the subgranular layer of the dentate gyrus. Glia. 2008;56(7):791-800.

Christensen LB, Woods TA, Carmody AB, Caughey B, Peterson KE. Age-related differences in neupro-inflammatory responses associated with a distinct profile of regulatory markers on neonatal microglia. J Neuroinflammation. 2014;11:70.

Chrysis D, Calikoglu AS, Ye P, D'Ercole AJ. Insulin-like growth factor-I overexpression attenuates cerebellar apoptosis by altering the expression of Bcl family proteins in a developmentally specific manner. J Neurosci. 2001;21(5):1481-9.

Chung JS, Dougherty I, Cruz PD Jr, Ariizumi K. Syndecan-4 mediates the coinhibitory function of DC-HIL on T cell activation. J Immunol. 2007;179(9):5778-84.

Colonna M, Butovsky O. Microglia Function in the Central Nervous System During Health and Neurodegeneration. Annu Rev Immunol. 2017.

Covey MV, Loporchio D, Buono KD, Levison SW. Opposite effect of inflammation on subventricular zone versus hippocampal precursors in brain injury. Ann Neurol. 2011;70(4):616-26.

Cunningham CL, Martínez-Cerdeño V, Noctor SC. Microglia regulate the number of neural precursor cells in the developing cerebral cortex. J Neurosci. 2013;33(10):4216-33.

Deierborg T, Roybon L, Inacio AR, Pesic J, Brundin P. Brain injury activates microglia that induce neural stem cell proliferation ex vivo and promote differentiation of neurosphere-derived cells into neurons and oligodendrocytes. Neuroscience. 2010;171(4):1386-96.

Del Rio-Hortega P. Microglia. In: Penfield W, editor. Cytology and Cellular Pathology of the Nervous System. New York: Hoeber; 1932, p. 482–1924–534.

Denker SP, Ji S, Dingman A, Lee SY, Derugin N, Wendland MF, Vexler ZS. Macrophages are comprised of resident brain microglia not infiltrating peripheral monocytes acutely after neonatal stroke. J Neurochem. 2007;100(4):893-904.

Ekdahl CT, Claasen JH, Bonde S, Kokaia Z, Lindvall O. Inflammation is detrimental for neurogenesis in adult brain. Proc Natl Acad Sci U S A. 2003;100(23):13632-7.

Erickson RI, Paucar AA, Jackson RL, Visnyei K, Kornblum H. Roles of insulin and transferrin in neural progenitor survival and proliferation. J Neurosci Res. 2008;86(8):1884-94.

Faustino JV, Wang X, Johnson CE, Klibanov A, Derugin N, Wendland MF, Vexler ZS. Microglial cells contribute to endogenous brain defences after acute neonatal focal stroke. J Neurosci. 2011;31(36):12992-3001.

Fernández-López D, Faustino J, Klibanov AL, Derugin N, Blanchard E, Simon F, Leib SL, Vexler ZS. Microglial Cells Prevent Hemorrhage in Neonatal Focal Arterial Stroke. J Neurosci. 2016;36(10):2881-93.

Ferrer I, Bernet E, Soriano E, del Rio T, Fonseca M. Naturally occurring cell death in the cerebral cortex of the rat and removal of dead cells by transitory phagocytes. Neuroscience. 1990;39(2):451-8.

Fleiss B, Gressens P. Tertiary mechanisms of brain damage: a new hope for treatment of cerebral palsy? Lancet Neurol. 2012;11(6):556-66.

Fourgeaud L, Través PG, Tufail Y, Leal-Bailey H, Lew ED, Burrola PG, Callaway P, Zagórska A, Rothlin CV, Nimmerjahn A, Lemke G.
TAM receptors regulate multiple features of microglial physiology. Nature. 2016;532(7598):240-4.

Freilich RW, Woodbury ME, Ikezu T. Integrated expression profiles of mRNA and miRNA in polarized primary murine microglia. PLoS One. 2013;8(11):e79416.

Fricker M, Oliva-Martín MJ, Brown GC. Primary phagocytosis of viable neurons by microglia activated with LPS or Aβ is dependent on calreticulin/LRP phagocytic signalling. J Neuroinflammation. 2012;9:196.

Frost JL, Schafer DP. Microglia: Architects of the Developing Nervous System. Trends Cell Biol. 2016;26(8):587-97.

Garcia-Bonilla L, Faraco G, Moore J, Murphy M, Racchumi G, Srinivasan J, Brea D, Iadecola C, Anrather J. Spatio-temporal profile, phenotypic diversity, and fate of recruited monocytes into the post-ischemic brain. J Neuroinflammation. 2016;13(1):285.

Gebara E, Sultan S, Kocher-Braissant J, Toni N. Adult hippocampal neurogenesis inversely correlates with microglia in conditions of voluntary running and aging. Front Neurosci. 2013;7:145.

Gemma C, Bachstetter AD, Cole MJ, Fister M, Hudson C, Bickford PC. Blockade of caspase-1 increases neurogenesis in the aged hippocampus. Eur J Neurosci. 2007;26(10):2795-803.

Ginhoux F, Greter M, Leboeuf M, Nandi S, See P, Gokhan S, Mehler MF, Conway SJ, Ng LG, Stanley ER, Samokhvalov IM, Merad M. Fate mapping analysis reveals that adult microglia derive from primitive macrophages. Science. 2010;330(6005):841-5.

Goings GE, Kozlowski DA, Szele FG. Differential activation of microglia in neurogenic versus non-neurogenic regions of the forebrain. Glia. 2006;54(4):329-42.

Hagberg H, Mallard C, Ferriero DM, Vannucci SJ, Levison SW, Vexler ZS, Gressens P. The role of inflammation in perinatal brain injury. Nat Rev Neurol. 2015;11(4):192-208.

Haile Y, Deng X, Ortiz-Sandoval C, Tahbaz N, Janowicz A, Lu JQ, Kerr BJ, Gutowski NJ, Holley JE, Eggleton P, Giuliani F, Simmen T. Rab32 connects ER stress to mitochondrial defects in multiple sclerosis. J Neuroinflammation. 2017;14(1):19.

Heldmann U, Mine Y, Kokaia Z, Ekdahl CT, Lindvall O. Selective depletion of Mac-1-expressing microglia in rat subventricular zone does not alter neurogenic response early after stroke. Exp Neurol. 2011;229(2):391-8.

Hellström-Erkenstam NH, Smith PL, Fleiss B, Nair S, Svedin P, Wang W, Boström M, Gressens P, Hagberg H, Brown KL, Sävman K, Mallard C. Temporal Characterization of Microglia/Macrophage Phenotypes in a Mouse Model of Neonatal Hypoxic-Ischemic Brain Injury. Front Cell Neurosci. 2016;10:286.

Hellwig S, Heinrich A, Biber K. The brain's best friend: microglial neurotoxicity revisited. Front Cell Neurosci. 2013;7:71.

Hodge RD, D'Ercole AJ, O'Kusky JR. Insulin-like growth factor-I accelerates the cell cycle by decreasing G1 phase length and increases cell cycle reentry in the embryonic cerebral cortex. J Neurosci. 2004;24(45):10201-10.

Holtman IR, Raj DD, Miller JA, Schaafsma W, Yin Z, Brouwer N, Wes PD, Möller T, Orre M, Kamphuis W, Hol EM, Boddeke EW, Eggen BJ. Induction of a common microglia gene expression signature by aging and neurodegenerative conditions: a co-expression meta-analysis. Acta Neuropathol Commun. 2015;3:31.

Hristova M, Cuthill D, Zbarsky V, Acosta-Saltos A, Wallace A, Blight K, Buckley SM, Peebles D, Heuer H, Waddington SN, Raivich G. Activation and deactivation of periventricular white matter phagocytes during postnatal mouse development. Glia. 2010;58(1):11-28.

Hu X, Leak RK, Shi Y, Suenaga J, Gao Y, Zheng P, Chen J. Microglial and macrophage polarization—new prospects for brain repair. Nat Rev Neurol. 2015;11(1):56-64.

Huang JJ, Ma WJ, Yokoyama S. Expression and immunolocalization of Gpnmb, a glioma-associated glycoprotein, in normal and inflamed central nervous systems of adult rats. Brain Behav. 2012;2(2):85-96.

Jang ES, Goldman JE. Pax6 expression is sufficient to induce a neurogenic fate in glial progenitors of the neonatal subventricular zone. PLoS One. 2011;6(6):e20894.

Kamphuis W, Kooijman L, Schetters S, Orre M, Hol EM. Transcriptional profiling of CD11c-positive microglia accumulating around amyloid plaques in a mouse model for Alzheimer's disease. Biochim Biophys Acta. 2016;1862(10):1847-60.

Kaur C, Rathnasamy G, Ling EA. Roles of activated microglia in hypoxia induced neuroinflammation in the developing brain and the retina. J Neuroimmune Pharmacol. 2013;8(1):66-78.

Kempermann G, Song H, Gage FH. Neurogenesis in the Adult Hippocampus. Cold Spring Harb Perspect Biol. 2015;7(9):a018812.

Kerrigan AM, Navarro-Nuñez L, Pyz E, Finney BA, Willment JA, Watson SP, Brown GD. Podoplanin-expressing inflammatory macrophages activate murine platelets via CLEC-2. J Thromb Haemost. 2012;10(3):484-6.

Kettenmann H, Hanisch UK, Noda M, Verkhratsky A. Physiology of microglia. Physiol Rev. 2011;91(2):461-553.

Khazipov R, Zaynutdinova D, Ogievetsky E, Valeeva G, Mitrukhina O, Manent JB, Represa A. Atlas of the Postnatal Rat Brain in Stereotaxic Coordinates. Front Neuroanat. 2015;9:161.

Khwaja O, Volpe JJ. Pathogenesis of cerebral white matter injury of prematurity. Arch Dis Child Fetal Neonatal Ed. 2008;93(2):F153-61.

Kim E, Cho S. Microglia and Monocyte-Derived Macrophages in Stroke. Neurotherapeutics. 2016;13(4):702-718.

Kim CC, Nakamura MC, Hsieh CL. Brain trauma elicits non-canonical macrophage activation states. J Neuroinflammation. 2016;13(1):117.

Kohman RA, DeYoung EK, Bhattacharya TK, Peterson LN, Rhodes JS. Wheel running attenuates microglia proliferation and increases expression of a proneurogenic phenotype in the hippocampus of aged mice. Brain Behav Immun. 2012;26(5):803-10.

Kurinczuk JJ, White-Koning M, Badawi N. Epidemiology of neonatal encephalopathy and hypoxic-ischaemic encephalopathy. Early Hum Dev. 2010;86(6):329-38.

Lalancette-Hébert M, Gowing G, Simard A, Weng YC, Kriz J. Selective ablation of proliferating microglial cells exacerbates ischemic injury in the brain. J Neurosci. 2007;27(10):2596-605.

Lawn JE, Cousens S, Zupan J; Lancet Neonatal Survival Steering Team. 4 million neonatal deaths: when? Where? Why? Lancet. 2005;365(9462):891-900.

Lawson LJ, Perry VH, Dri P, Gordon S. Heterogeneity in the distribution and morphology of microglia in the normal adult mouse brain. Neuroscience. 1990;39(1):151-70.

Li L, Walker TL, Zhang Y, Mackay EW, Bartlett PF. Endogenous interferon gamma directly regulates neural precursors in the non-inflammatory brain. J Neurosci. 2010;30(27):9038-50.

Liang Y, Lin S, Zou L, Zhou H, Zhang J, Su B, Wan Y. Expression profiling of Rab GTPases reveals the involvement of Rab20 and Rab32 in acute brain inflammation in mice. Neurosci Lett. 2012;527(2):110-4.

Ling EA, Wong WC. The origin and nature of ramified and amoeboid microglia: a historical review and current concepts. Glia. 1993;7(1):9-18.

Liu J, Hjorth E, Zhu M, Calzarossa C, Samuelsson EB, Schultzberg M, Åkesson E. Interplay between human microglia and neural stem/progenitor cells in an allogeneic co-culture model. J Cell Mol Med. 2013;17(11):1434-43.

Lu Z, Elliott MR, Chen Y, Walsh JT, Klibanov AL, Ravichandran KS, Kipnis J. Phagocytic activity of neuronal progenitors regulates adult neurogenesis. Nat Cell Biol. 2011;13(9):1076-83.

Marín-Teva JL, Dusart I, Colin C, Gervais A, van Rooijen N, Mallat M. Microglia promote the death of developing Purkinje cells. Neuron. 2004;41(4):535-47.

Marshall GP 2nd, Demir M, Steindler DA, Laywell ED. Subventricular zone microglia possess a unique capacity for massive in vitro expansion. Glia. 2008;56(16):1799-808.

Marshall GP 2nd, Deleyrolle LP, Reynolds BA, Steindler DA, Laywell ED. Microglia from neurogenic and non-neurogenic regions display differential proliferative potential and neuroblast support. Front Cell Neurosci. 2014;8:180.

Matcovitch-Natan O, Winter DR, Giladi A, Vargas Aguilar S, Spinrad A, Sarrazin S, Ben-Yehuda H, David E, Zelada González F, Perrin P, Keren-Shaul H, Gury M, Lara-Astaiso D, Thaiss CA, Cohen M, Bahar Halpern K, Baruch K, Deczkowska A, Lorenzo-Vivas E, Itzkovitz S, Elinav E,
Sieweke MH, Schwartz M, Amit I. Microglia development follows a stepwise program to regulate brain homeostasis. Science. 2016;353(6301):aad8670.

McKercher SR, Torbett BE, Anderson KL, Henkel GW, Vestal DJ, Baribault H, Klemsz M, Feeney AJ, Wu GE, Paige CJ, Maki RA. Targeted disruption of the PU.1 gene results in multiple hematopoietic abnormalities. EMBO J. 1996;15(20):5647-58.

Mildner A, Schmidt H, Nitsche M, Merkler D, Hanisch UK, Mack M, Heikenwalder M, Brück W, Priller J, Prinz M. Microglia in the adult brain arise from Ly-6ChiCCR2+ monocytes only under defined host conditions. Nat Neurosci. 2007;10(12):1544-53.

Mittelbronn M, Dietz K, Schluesener HJ, Meyermann R. Local distribution of microglia in the normal adult human central nervous system differs by up to one order of magnitude. Acta Neuropathol. 2001;101(3):249-55.

Monier A, Adle-Biassette H, Delezoide AL, Evrard P, Gressens P, Verney C. Entry and distribution of microglial cells in human embryonic and fetal cerebral cortex. J Neuropathol Exp Neurol. 2007;66(5):372-82.

Monje ML, Toda H, Palmer TD. Inflammatory blockade restores adult hippocampal neurogenesis. Science. 2003;302(5651):1760-5.

Morganti JM, Riparip LK, Rosi S. Call Off the Dog(ma): M1/M2 Polarization Is Concurrent following Traumatic Brain Injury. PLoS One. 2016;11(1):e0148001.

Morsch M, Radford R, Lee A, Don EK, Badrock AP, Hall TE, Cole NJ, Chung R. In vivo characterization of microglial engulfment of dying neurons in the zebrafish spinal cord. Front Cell Neurosci. 2015;9:321.

Mosher KI, Andres RH, Fukuhara T, Bieri G, Hasegawa-Moriyama M, He Y, Guzman R, Wyss-Coray T. Neural progenitor cells regulate microglia functions and activity. Nat Neurosci. 2012;15(11):1485-7.

Nakano Y, Suzuki Y, Takagi T, Kitashoji A, Ono Y, Tsuruma K, Yoshimura S, Shimazawa M, Iwama T, Hara H. Glycoprotein nonmetastatic melanoma protein B (GPNMB) as a novel neuroprotective factor in cerebral ischemia-reperfusion injury. Neuroscience. 2014;277:123-31.

Neumann H, Kotter MR, Franklin RJ. Debris clearance by microglia: an essential link between degeneration and regeneration. Brain. 2009;132(Pt 2):288-95.

Nguyen A, Armstrong EA, and Yager JY. Unilateral Common Carotid Artery Ligation as a Modelof Perinatal Asphyxia: The Original Rice–Vannucci Model. In: Yager JY, editor. Animal Models of Neurodevelopmental Disorders, Neuromethods, Vol. 104. Springer New York Heidelberg Dordrecht London; 2015. p.1-13.

Nimmerjahn A, Kirchhoff F, Helmchen F. Resting microglial cells are highly dynamic surveillants of brain parenchyma in vivo. Science. 2005;308(5726):1314-8.

Ong J, Plane JM, Parent JM, Silverstein FS. Hypoxic-ischemic injury stimulates subventricular zone proliferation and neurogenesis in the neonatal rat. Pediatr Res. 2005;58(3):600-6.

Ortega FJ, Vukovic J, Rodríguez MJ, Bartlett PF. Blockade of microglial KATP -channel abrogates suppression of inflammatory-mediated inhibition of neural precursor cells. Glia. 2014;62(2):247-58.

Paolicelli RC, Bolasco G, Pagani F, Maggi L, Scianni M, Panzanelli P, Giustetto M, Ferreira TA, Guiducci E, Dumas L, Ragozzino D, Gross CT. Synaptic pruning by microglia is necessary for normal brain development. Science. 2011;333(6048):1456-8.

Parent JM, Vexler ZS, Gong C, Derugin N, Ferriero DM. Rat forebrain neurogenesis and striatal neuron replacement after focal stroke. Ann Neurol. 2002;52(6):802-13.

Parkhurst CN, Yang G, Ninan I, Savas JN, Yates JR 3rd, Lafaille JJ, Hempstead BL, Littman DR, Gan WB. Microglia promote learning-dependent synapse formation through brain-derived neurotrophic factor. Cell. 2013;155(7):1596-609.

Pereira L, Medina R, Baena M, Planas AM, Pozas E. IFN gamma regulates proliferation and neuronal differentiation by STAT1 in adult SVZ niche. Front Cell Neurosci. 2015;9:270.

Perry VH, Hume DA, Gordon S. Immunohistochemical localization of macrophages and microglia in the adult and developing mouse brain. Neuroscience. 1985;15(2):313-26.

Pimentel-Coelho PM, Santiago MF and Mendez-Otero R. Future Perspectives for the Treatment of Neonatal Hypoxic-Ischemic Encephalopathy. In: Tanasescu R, editor. Miscellanea on Encephalopathies - A Second Look. InTech, Rijeka, Croatia; 2012. p. 243- 266.

Plane JM, Liu R, Wang TW, Silverstein FS, Parent JM. Neonatal hypoxic-ischemic injury increases forebrain subventricular zone neurogenesis in the mouse. Neurobiol Dis. 2004;16(3):585-95.

Priller J, Flügel A, Wehner T, Boentert M, Haas CA, Prinz M, Fernández-Klett F, Prass K, Bechmann I, de Boer BA, Frotscher M, Kreutzberg GW, Persons DA, Dirnagl U. Targeting gene-modified hematopoietic cells to the central nervous system: use of green fluorescent protein uncovers microglial engraftment. Nat Med. 2001;7(12):1356-61.

Przanowski P, Dabrowski M, Ellert-Miklaszewska A, Kloss M, Mieczkowski J, Kaza B, Ronowicz A, Hu F, Piotrowski A, Kettenmann H, Komorowski J, Kaminska B. The signal transducers Stat1 and Stat3 and their novel target Jmjd3 drive the expression of inflammatory genes in microglia. J Mol Med (Berl). 2014;92(3):239-54.

Rahpeymai Y, Hietala MA, Wilhelmsson U, Fotheringham A, Davies I, Nilsson AK, Zwirner J, Wetsel RA, Gerard C, Pekny M, Pekna M. Complement: a novel factor in basal and ischemia-induced neurogenesis. EMBO J. 2006;25(6):1364-74.

Ransohoff RM. A polarizing question: do M1 and M2 microglia exist? Nat Neurosci. 2016;19(8):987-91.

Rice JE 3rd, Vannucci RC, Brierley JB. The influence of immaturity on hypoxic-ischemic brain damage in the rat. Ann Neurol. 1981;9(2):131-41.

Ripoll VM, Irvine KM, Ravasi T, Sweet MJ, Hume DA. Gpnmb is induced in macrophages by IFN-gamma and lipopolysaccharide and acts as a feedback regulator of ppro-inflammatory responses. J Immunol. 2007;178(10):6557-66.

Ritzel RM, Patel AR, Grenier JM, Crapser J, Verma R, Jellison ER, McCullough LD. Functional differences between microglia and monocytes after ischemic stroke. J Neuroinflammation. 2015;12:106.

Saba R, Gushue S, Huzarewich RL, Manguiat K, Medina S, Robertson C, Booth SA. MicroRNA 146a (miR-146a) is over-expressed during prion disease and modulates the innate immune response and the microglial activation state. PLoS One. 2012;7(2):e30832.

Sato K. Effects of Microglia on Neurogenesis. Glia. 2015;63(8):1394-405.

Schafer DP, Lehrman EK, Kautzman AG, Koyama R, Mardinly AR, Yamasaki R, Ransohoff RM, Greenberg ME, Barres BA, Stevens B. Microglia sculpt postnatal neural circuits in an activity and complement-dependent manner. Neuron. 2012;74(4):691-705.

Schulz C, Gomez Perdiguero E, Chorro L, Szabo-Rogers H, Cagnard N, Kierdorf K, Prinz M, Wu B, Jacobsen SE, Pollard JW, Frampton J, Liu KJ, Geissmann F. A lineage of myeloid cells independent of Myb and hematopoietic stem cells. Science. 2012;336(6077):86-90.

Shankaran S, Pappas A, McDonald SA, Vohr BR, Hintz SR, Yolton K, Gustafson KE, Leach TM, Green C, Bara R, Petrie Huitema CM, Ehrenkranz RA, Tyson JE, Das A, Hammond J, Peralta-Carcelen M, Evans PW, Heyne RJ, Wilson-Costello DE, Vaucher YE, Bauer CR, Dusick AM, Adams-Chapman I, Goldstein RF, Guillet R, Papile LA, Higgins RD; Eunice Kennedy Shriver NICHD Neonatal Research Network. Childhood outcomes after hypothermia for neonatal encephalopathy. N Engl J Med. 2012;366(22):2085-92.

Shevell MI, Majnemer A, Rosenbaum P, Abrahamowicz M. Etiologic yield of subspecialists' evaluation of young children with global developmental delay. J Pediatr. 2000;136(5):593-8.

Shigemoto-Mogami Y, Hoshikawa K, Goldman JE, Sekino Y, Sato K. Microglia enhance neurogenesis and oligodendrogenesis in the early postnatal subventricular zone. J Neurosci. 2014;34(6):2231-43.

Sierra A, Encinas JM, Deudero JJ, Chancey JH, Enikolopov G, Overstreet-Wadiche LS, Tsirka SE, Maletic-Savatic M. Microglia shape adult hippocampal neurogenesis through apoptosis-coupled phagocytosis. Cell Stem Cell. 2010;7(4):483-95.

Sierra A, Abiega O, Shahraz A, Neumann H. Janus-faced microglia: beneficial and detrimental consequences of microglial phagocytosis. Front Cell Neurosci. 2013;7:6.

Solga AC, Pong WW, Walker J, Wylie T, Magrini V, Apicelli AJ, Griffith M, Griffith OL, Kohsaka S, Wu GF, Brody DL, Mardis ER, Gutmann DH. RNA-sequencing reveals oligodendrocyte and neuronal transcripts in microglia relevant to central nervous system disease. Glia. 2015;63(4):531-48.

Squarzoni P, Oller G, Hoeffel G, Pont-Lezica L, Rostaing P, Low D, Bessis A, Ginhoux F, Garel S. Microglia modulate wiring of the embryonic forebrain. Cell Rep. 2014;8(5):1271-9.

Srinivasan K, Friedman BA, Larson JL, Lauffer BE, Goldstein LD, Appling LL, Borneo J, Poon C, Ho T, Cai F, Steiner P, van der Brug MP, Modrusan Z, Kaminker JS, Hansen DV. Untangling the brain's neuro-inflammatory and neurodegenerative transcriptional responses. Nat Commun. 2016;7:11295.

Supeno NE, Pati S, Hadi RA, Ghani AR, Mustafa Z, Abdullah JM, Idris FM, Han X, Jaafar H. IGF-1 acts as controlling switch for long-term proliferation and maintenance of EGF/FGF-responsive striatal neural stem cells. Int J Med Sci. 2013;10(5):522-31.

Szalay G, Martinecz B, Lénárt N, Környei Z, Orsolits B, Judák L, Császár E, Fekete R, West BL, Katona G, Rózsa B, Dénes Á. Microglia protect against brain injury and their selective elimination dysregulates neuronal network activity after stroke. Nat Commun. 2016;7:11499.

Szulzewsky F, Pelz A, Feng X, Synowitz M, Markovic D, Langmann T, Holtman IR, Wang X, Eggen BJ, Boddeke HW, Hambardzumyan D, Wolf SA, Kettenmann H. Glioma-associated microglia/macrophages display an expression profile different from M1 and M2 polarization and highly express Gpnmb and Spp1. PLoS One. 2015;10(2):e0116644.

Takahashi K, Rochford CD, Neumann H. Clearance of apoptotic neurons without inflammation by microglial triggering receptor expressed on myeloid cells-2. J Exp Med. 2005;201(4):647-57.

Talaverón R, Fernández P, Escamilla R, Pastor AM, Matarredona ER, Sáez JC. Neural progenitor cells isolated from the subventricular zone present hemichannel activity and form functional gap junctions with glial cells. Front Cell Neurosci. 2015;9:411.

Tanaka H, Shimazawa M, Kimura M, Takata M, Tsuruma K, Yamada M, Takahashi H, Hozumi I, Niwa J, Iguchi Y, Nikawa T, Sobue G, Inuzuka T, Hara H. The potential of GPNMB as novel neuroprotective factor in amyotrophic lateral sclerosis. Sci Rep. 2012;2:573.

Thored P, Arvidsson A, Cacci E, Ahlenius H, Kallur T, Darsalia V, Ekdahl CT, Kokaia Z, Lindvall O. Persistent production of neurons from adult brain stem cells during recovery after stroke. Stem Cells. 2006;24(3):739-47.

Thored P, Heldmann U, Gomes-Leal W, Gisler R, Darsalia V, Taneera J, Nygren JM, Jacobsen SE, Ekdahl CT, Kokaia Z, Lindvall O. Long-term accumulation of microglia with proneurogenic phenotype concomitant with persistent neurogenesis in adult subventricular zone after stroke. Glia. 2009;57(8):835-49.

Tremblay ME, Lowery RL, Majewska AK: Microglial interactions with synapses are modulated by visual experience. PLoS Biol. 2010;8(11):e1000527

Tuor UI, Simone CS, Barks JD, Post M. Dexamethasone prevents cerebral infarction without affecting cerebral blood flow in neonatal rats. Stroke. 1993;24(3):452-7.

Ueno M, Fujita Y, Tanaka T, Nakamura Y, Kikuta J, Ishii M, Yamashita T. Layer V cortical neurons require microglial support for survival during postnatal development. Nat Neurosci. 2013;16(5):543-51.

Uhrin P, Perkmann T, Binder B, Schabbauer G. ISG12 is a critical modulator of innate immune responses in murine models of sepsis. Immunobiology. 2013;218(9):1207-16.

Umekawa T, Osman AM, Han W, Ikeda T, Blomgren K. Resident microglia, rather than blood-derived macrophages, contribute to the earlier and more pronounced inflammatory reaction in the immature compared with the adult hippocampus after hypoxia-ischemia. Glia. 2015;63(12):2220-30.

Vexler ZS, Yenari MA. Does inflammation after stroke affect the developing brain differently than adult brain? Dev Neurosci. 2009;31(5):378-93.

Vukovic J, Colditz MJ, Blackmore DG, Ruitenberg MJ, Bartlett PF. Microglia modulate hippocampal neural precursor activity in response to exercise and aging. J Neurosci. 2012;32(19):6435-43.

Wake H, Moorhouse AJ, Jinno S, Kohsaka S, Nabekura J. Resting microglia directly monitor the functional state of synapses in vivo and determine the fate of ischemic terminals. J Neurosci. 2009;29(13):3974-80.

Wakselman S, Béchade C, Roumier A, Bernard D, Triller A, Bessis A. Developmental neuronal death in hippocampus requires the microglial CD11b integrin and DAP12 immunoreceptor. J Neurosci. 2008;28(32):8138-43.

Walton NM, Sutter BM, Laywell ED, Levkoff LH, Kearns SM, Marshall GP 2nd, Scheffler B, Steindler DA. Microglia instruct subventricular zone neurogenesis. Glia. 2006;54(8):815-25.

Williamson LL, Chao A, Bilbo SD. Environmental enrichment alters glial antigen expression and neuroimmune function in the adult rat hippocampus. Brain Behav Immun. 2012;26(3):500-10.

Winerdal M, Winerdal ME, Kinn J, Urmaliya V, Winqvist O, Adén U. Long lasting local and systemic inflammation after cerebral hypoxic ischemia in newborn mice. PLoS One. 2012;7(5):e36422.

Wu CH, Wen CY, Shieh JY, Ling EA. A quantitative and morphometric study of the transformation of amoeboid microglia into ramified microglia in the developing corpus callosum in rats. J Anat. 1992;181:423-30.

Yang Z, Levison SW. Hypoxia/ischemia expands the regenerative capacity of progenitors in the perinatal subventricular zone. Neuroscience. 2006;139(2):555-64.

Yasuda M, Tanaka Y, Omodaka K, Nishiguchi KM, Nakamura O, Tsuda S, Nakazawa T. Transcriptome profiling of the rat retina after optic nerve transection. Sci Rep. 2016;6:28736.

Yeo YA, Martínez Gómez JM, Croxford JL, Gasser S, Ling EA, Schwarz H. CD137 ligand activated microglia induces oligodendrocyte apoptosis via reactive oxygen species. J Neuroinflammation. 2012;9:173. doi: 10.1186/1742-2094-9-173.

Zhang RL, Zhang ZG, Chopp M. Ischemic stroke and neurogenesis in the subventricular zone. Neuropharmacology. 2008;55(3):345-52.

Zhang S, Yu M, Guo Q, Li R, Li G, Tan S, Li X, Wei Y, Wu M. Annexin A2 binds to endosomes and negatively regulates TLR4-triggered inflammatory responses via the TRAM-TRIF pathway. Sci Rep. 2015;5:15859.

9. Abbreviations

AD	Alzheimer's disease
ALS	Amyotrophic lateral sclerosis
Arg1	Arginase-1
BBB	Blood-brain-barrier
BDNF	Brain-derived neurotrophic factor
BM	Bone marrow
BRDU	Bromodeoxyuridine
CAA	Common carotid artery
CC	Median corpus callosum
CC3	Cleaved-caspase-3
CI	95% confidence interval
CNS	Central nervous system
CSF1R	Colony stimulating factor 1 receptor
CR3	Complement receptor 3
CX	M2 supplementary motor cortex
CX3CL1	Fractalkine
CX3CR1	Fractalkine receptor
DAP12	TYRO protein tyrosine kinase-binding protein
DIC	Days in culture
E	Embryonic day
EDTA	Ethylene-diaminetetraacetic acid
EGF	Epidermal growth factor
FC	Fold-change
FDR	False discovery rate
FGF	Fibroblast growth factor
HBSS	Hank's balanced salt solution
HI	Hypoxia-ischemia
HIE	Hypoxic-ischemic encephalopathy
Iba1	Ionized calcium-binding adapter molecule 1
iDTR	Inducible diphtheria toxin receptor
iNOS	Inducible nitric oxidase
IFN-γ	Interferon-γ
IGF-1	Insulin growth factor-1
IHC	Immunohistochemical
IL	Interleukin
KEGG	Kyoto Encyclopedia of Genes and Genomes
LPS	Lipopolysaccharide
MCAO	Middle cerebral artery occlusion
NADPH	Nicotinamide adenine dinucleotide phosphate
NPC	Neural progenitor cell
NSC	Neural stem cell
P	Postnatal day
PAX6	Paired box 6 protein
PB	Phosphate buffer
PBS	Phosphate-buffered saline
PCNA	Proliferating cell nuclear antigen
PFA	Paraformaldehyde
PSA-NCAM	Polysialylated-neural cell adhesion molecule
qRT-PCR	Quantitative real-time polymerase chain reaction
RT	Room temperature
SD	Standard deviation
SGZ	Subgranular zone
SOX2	Sex determining region Y-box 2
SVZ	Subventricular zone
TBS	Tris-buffered saline
TGF-β	Transforming growth factor-β
TMEM119	Transmembrane protein 119
TNF-α	Tumor necrosis factor-α
TUJ1	Neuron-specific class III β -tubulin
TREM-2	Triggering receptor expressed on myeloid cells-2
VEGF	Vascular endothelial growth factor